# APPENDIX A

# Impact of Urbanization on the Hydrology of the Pocono Creek Watershed: A Model Study

United States
Environmental Protection
Agency

# Final Report

# Impact of Urbanization on the Hydrology of the Pocono Creek Watershed: A Model Study

**EPA Report number #**
**September 2006**

# Impact of Urbanization on the Hydrology of Pocono Creek Watershed: A Model Study

By

Mohamed M. Hantush
U.S. Environmental Protection Agency
Cincinnati, Ohio 45268

Latif Kalin
Oak Ridge Institute for Science and Education (ORISE)
U.S. Environmental Protection Agency
Cincinnati, Ohio 45268

National Risk Management Research Laboratory
Office of Research and Development
U.S. Environmental Protection Agency
Cincinnati, Ohio 45268

# Notice

The U.S. Environmental Protection Agency through its Office of Research and Development funded the research described here. It has been subjected to the Agency's peer and administrative review and has been approved for publication as an EPA document.

This research was supported in part by an appointment to the Post Doctoral Research Program at the National Risk Management Research Laboratory, administered by the Oak Ridge Institute for Science and Education through Interagency Agreement No. DW89939836 between the U.S. Department of Energy and the U.S. Environmental Protection Agency. Mention of trade names or commercial products does not constitute endorsement or recommendation for use.

All research projects making conclusions or recommendations based on environmentally related measurements and funded by the Environmental Protection Agency are required to comply with the Agency Quality Assurance Program. This report has been subjected to QA/QC review. The report presented a mathematical framework for modeling hydrology of a watershed and did not involve collection and analysis of environmental measurements.

# Foreword

The U.S. Environmental Protection Agency (EPA) is charged by Congress with protecting the Nation's land, air, and water resources. Under a mandate of national environmental laws, the Agency strives to formulate and implement actions leading to a compatible balance between human activities and the ability of natural systems to support and nurture life. To meet this mandate, EPA's research program is providing data and technical support for solving environmental problems today and building a science knowledge base necessary to manage our ecological resources wisely, understand how pollutants affect our health, and prevent or reduce environmental risks in the future.

The National Risk Management Research Laboratory (NRMRL) is the Agency's center for investigation of technological and management approaches for preventing and reducing risks from pollution that threaten human health and the environment. The focus of the Laboratory's research program is on methods and their cost-effectiveness for prevention and control of pollution to air, land, water, and subsurface resources; protection of water quality in public water systems; remediation of contaminated sites, sediments and ground water; prevention and control of indoor air pollution; and restoration of ecosystems. NRMRL collaborates with both public and private sector partners to foster technologies that reduce the cost of compliance and to anticipate emerging problems. NRMRL's research provides solutions to environmental problems by: developing and promoting technologies that protect and improve the environment; advancing scientific and engineering information to support regulatory and policy decisions; and providing the technical support and information transfer to ensure implementation of environmental regulations and strategies at the national, state, and community levels.

This publication has been produced as part of the Laboratory's strategic long-term research plan. It is published and made available by EPA's Office of Research and Development to assist the user community and to link researchers with their clients.

**Sally Gutierrez, Director**
**National Risk Management Research Laboratory**

# Abstract

The Pocono Creek watershed located in Monroe County, PA, is threatened by high population growth and urbanization. Of concern specifically is the potential impact of future developments in the watershed on the reduction of base flow and the consequent risk of degradation of wild brown trout habitats in Pocono Creek. Anticipated increase in imperviousness, on the other hand, is expected to elevate flood risk and the associated environmental damage. A watershed hydrology based modeling study was initiated by the U.S. EPA in collaboration with the U.S. Geological Survey and the Pennsylvania Fish and Boat Commission to assist Monroe County in planning for sustainable future development in the Pocono Creek watershed.

The Soil and Water Assessment Tool (SWAT) is selected to model the impact of projected future build out in the Pocono Creek watershed on the hydrologic response thereof. The model is successfully calibrated and validated for two sources of precipitation data, raingauge and Next Generation Weather Radar (NEXRAD) hourly precipitation data. The results clearly show that NEXRAD is an effective and economic alternative source of spatio-temporal precipitation, and that future modeling studies in ungauged watersheds may benefit from the use of NEXRAD rainfall data.

Ensemble model forecast is constructed using time series analysis and Monte Carlo (MC) simulations to evaluate model predictive uncertainty. The MC simulations over a 20-year long period yielded an ensemble of rating curves of which the median and 95% confidence band of daily streamflows are plotted. These plots allow for the construction of the 95% confidence band for design flows corresponding to any given recurrence or return period. SWAT simulated daily streamflow rates in the range 2 to 11 ($m^3/s$) show the least uncertainty. Computed daily streamflow rates below 2 $m^3/s$ have the greatest uncertainty, whereas for flows higher than 11 $m^3/s$ uncertainty is moderate.

MC simulations over a 20-year period predict that, on the average, daily base flow would be reduced by 31% based on the projected build out in the watershed. The computed low-flow index, 7Q10, is expected to decline by 11%, and the monthly median daily flow is expected to be reduced by 10% on the average. The monthly peak of simulated daily flows and annual maximum daily flow on the average are predicted to increase by 21% and 19%, respectively. Watershed-averaged groundwater recharge is predicted to decline by 31% due to the projected land use changes. The median of the MC simulated flow duration curves shows that in general the likelihood that the watershed will experience high and low streamflows will increase with the projected urbanization.

An index methodology is developed to rank seven subwatersheds composing the modeled portion of the Pocono Creek watershed based on their relative impact on watershed response to anticipated land developments. The first index, $\alpha$, signifies the absolute impact of a particular catchment area on the watershed response. The second index, $\beta$, is $\alpha$ normalized by the percentage area of the sub-catchment, and therefore describes the impact per area of land use changes. With a few exceptions, $\alpha$ and $\beta$ indices produce similar rankings among

the 7 catchment areas for 7Q10, monthly median of daily flow, and annual maximum daily flow. These ranking results may be related to groundwater recharge, area, topographic features, and proximity to the streamflow gauge station. The very downstream catchment area 7 ranked first in terms of impact on annual maximum daily flows, and second in terms of impact on 7Q10 and monthly median daily flows. Catchment area 4 associated with the highest groundwater recharge was ranked first and second for impact on 7Q10 based on $\alpha$ and $\beta$ indices, respectively. Areas characterized by steep topography and intense wetlands ranked low, some times the lowest, with respect to impact on the three design flows.

The results of this model study point toward significant changes in low as well as high flow regimes, should the Pocono Creek watershed experience land use changes consistent with the projected build out in the watershed. Management measures may be taken in the future to minimize the predicted changes in the watershed hydrology.

# Table of Contents

# Figures

# Tables

# Acknowledgments

The U.S. Environmental Protection Agency, through its Office of Research and Development, funded the research described here through in-house efforts and in part by an appointment to the Postgraduate Research Program at the National Risk Management Research Laboratory administered by the Oak Ridge Institute for Science and Education through an interagency agreement between the U.S. Department of Energy and the U.S. Environmental Protection Agency. The report benefited from the constructive review comments of Dennis Lai and Rao S. Govindaraju.

# 1 Introduction

## 1.1 Pocono Creek Watershed

Pocono Creek watershed is a 46.5 square miles (120 $km^2$) basin located in Monroe County in Eastern Pennsylvania near the New Jersey border (Figure 1). The watershed drains into one of the main tributaries of Delaware River and has very good water and biological quality, and is designated as Special Protection Waters by the State and the Delaware River Basin Commission (DRBC). Wild brown trout population, tourism and significant outdoor recreation are major economic drivers of the area. Monroe County has the second fastest growing population in the state of Pennsylvania. The county is threatened by high population growth because of its attractive, pristine natural resources, and its proximity to the New York City and Philadelphia metropolitan regions. Since 1980 the population of Monroe County has nearly doubled and is projected to grow an additional 60% by 2020. Potential impacts, among others, include a degradation and loss of the forested and agricultural lands and deterioration of the local quality of life. Specifically, the concern is that the projected growth and land use changes along with the accompanying increased groundwater withdrawals in the watershed could well exceed sustainable levels, depleting groundwater and streamflows, and resulting in the loss of the Creek's wild brown trout. Anticipated increase of imperviousness due to urbanization in the watershed and projected increase in the demand for ground water due to the anticipated population growth threaten the sustainability of current base flows. Further, reduced infiltration and increased runoff rates have the potential to elevate peak flows and increase flood hazards during large storm events.

The Delaware River Basin Commission in collaboration with the U.S. Environmental Protection Agency (USEPA), Broadhead Watershed Association, Monroe County Conservation District, Monroe County Planning Commission, U.S. Geological Survey (USGS), and other stakeholders formed a consortium to study the potential future impacts of the projected growth and land use changes on the sustainability of the natural resources in the Pocono Creek watershed. The goals are to manage flows and growth in the Pocono Creek watershed such that natural resources are sustainable. The goals will be partly achieved through three integrated model studies by the USEPA, the U.S. Geological Survey (USGS), and the PA Fish and Boat Commission (PA F&B). These model studies will evaluate the effects of growth and land use change on ground water, streamflow, and the habitat of Pocono Creek. This report documents the development of the Pocono Creek Watershed model by the USEPA using the Soil and Water Assessment Tool (SWAT), its application to assess the impact of projected urbanization on streamflow characteristics, and identification of critical areas within the watershed having major contributions to changes in the streamflow. The results of this model study will be linked to a USGS groundwater flow model (MODFLOW) and the Pennsylvania Instream Flow Model (PIFM).

Distributed watershed models are utilized to better understand the role of hydrological processes that govern surface and subsurface water movement. They provide tools for environmental decision making and water resources planning and management. They are not

only helpful in making model predictions of future flow conditions, but also in assessment of hydrologic impacts of management measures scenarios, land cover and climate changes.

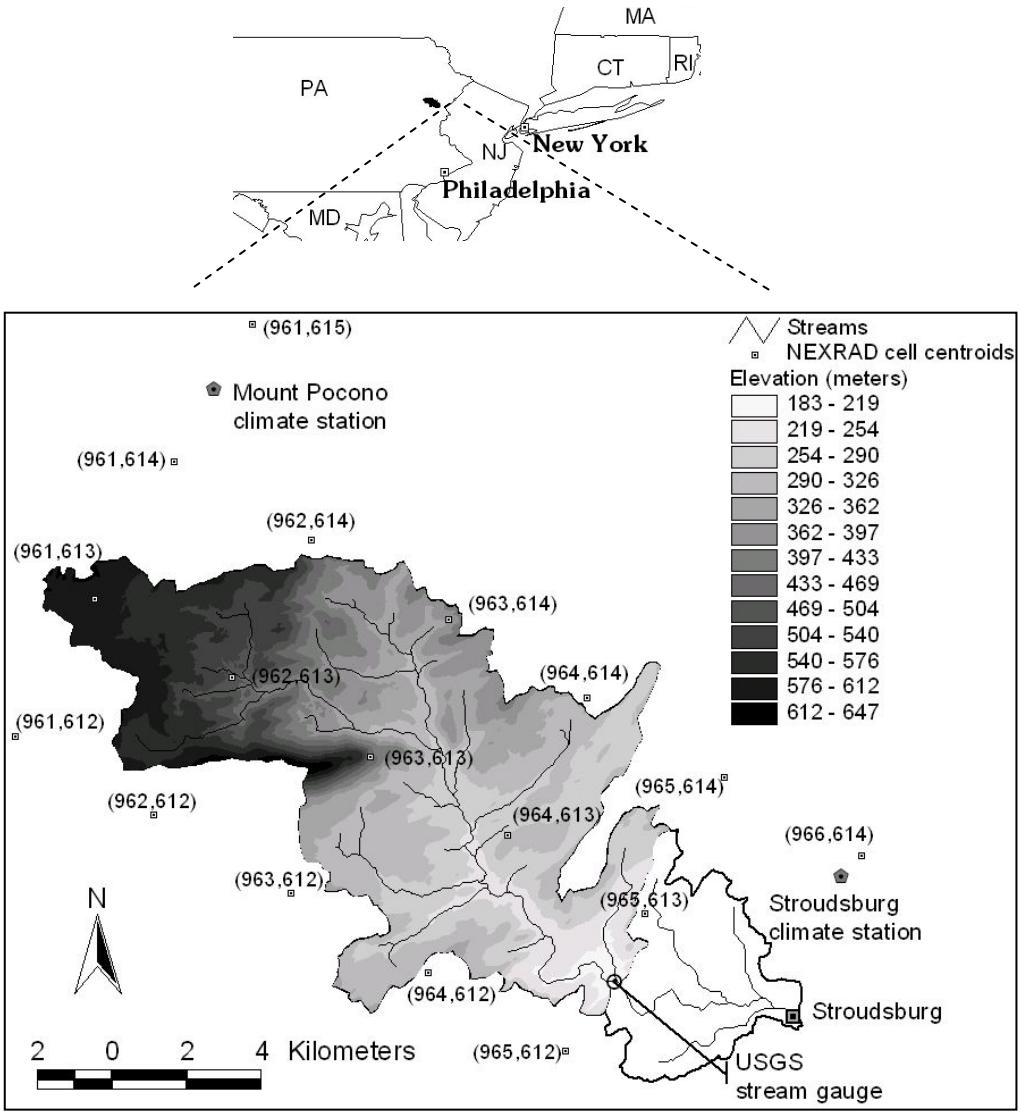


Figure 1. Pocono Creek Watershed: Location, topography, USGS stream gauge, climate stations and NEXRAD cell centroids (adapted from Kalin and Hantush, 2006a).

## 1.2 Objectives

The goal of the current model study and those by the USGS and the PA F&B, is to provide the necessary science so that Monroe County and stakeholders can make informed decisions that will assist them in developing and implementing sustainable water resources management strategies without compromising the integrity of the watershed's habitat. To

accomplish this overall goal, a watershed model is developed by the U.S. EPA to achieve the following objectives:

1- Calibrate and validate a watershed model for Pocono Creek Watershed and examine model performance with Next Generation Weather Radar (NEXRAD) data against that based on surface raingauge precipitation data: The distributed hydrologic Soil Water Assessment Tool (SWAT) will be calibrated and validated. Radar generated precipitation estimates such as from NEXRAD products have found increasing usage in the hydrologic community lately as an alternative source to gauge data. NEXRAD data can provide information about the spatial distribution of precipitation patterns. If proven successful, NEXRAD data can be a cost-effective alternative to the rather more costly and sparse raingauge data.

2- Predict the impact of projected land use changes on annual average recharge distribution: Spatial distribution of annual groundwater recharge rates will be computed pre- and after urbanization build out for use by a USGS MODFLOW model to simulate the impact of projected increase in groundwater withdrawals on base-flow reductions.

3- Predict the impact of projected land use changes on monthly median daily flows: Monthly median daily flows will be computed pre and post urbanization build out for use by the PIFM model which will be used to establish a relationship between flow reductions and potential habitat degradation in the Pocono Creek watershed.

4- Evaluate model predictive uncertainty: It is a common practice to calibrate and validate hydrologic and water quality models, but their forecasting abilities are rarely rigorously evaluated. In this modeling effort, the extra step of evaluating model error propagation will be conducted using time series analysis and Monte Carlo (MC) type simulations.

5- Compute the effect of urbanization on streamflow characteristics: It is anticipated that projected population growth and urbanization in Pocono Creek will be accompanied by an increase in impervious fraction of the watershed. The impact of land-use changes on low, high, monthly average, and median flows will be particularly investigated, along with 95% confidence band of the computed changes in flow characteristics.

6- Identify critical areas in the watershed: Once potential changes in flow characteristics are predicted by the watershed model due to projected land-use changes, the inner catchments contributing most of the changes will be identified using an index-based methodology.

### 1.3 Report Organization

This report is organized as follows. In Section 2 the rationale for the selection of the SWAT model to investigate the hydrology of Pocono Creek is established. A summary of model representation of the most important components of the hydrologic cycle and related parameters is presented. This summary is intended to define key model parameters and provide insights into the process of model calibration. Section 3 describes the study area,

model data and sources, and model calibration and validation using raingauge and NEXRAD precipitation data. The viability of NEXRAD technology as an alternative to raingauge networks as a source of spatio-temporal precipitation is established in the section. Error propagation and model forecast capability is investigated in Section 4 using time series analysis and Latin Hypercube Monte Carlo (MC) simulations. Section 5 explores potential impacts of projected build out in the watershed on changes in key streamflow characteristics using MC simulations. The impact of land use changes on (low, medium, and high) flow frequency and duration is also investigated. Section 6 applies an index approach to identify and rank subwatersheds or areas within subwatersheds that may contribute mostly to predicted changes in streamflow characteristics. Each section ends with conclusions. The final summary and conclusions of this model study appear in Section 7. References are included in Section 8.

## 1.4 Summary

Pocono Creek watershed is threatened by high population growth and urbanization. Potential impacts include degradation and loss of the forested and agricultural lands and deterioration of the local quality of life. The condition of the wild brown trout habitat has been identified as an indicator of the health of the watershed. Of specific concern is the potential impact of projected population growth and land use change on the reduction of base flow and the impact this may have on the degradation of wild brown trout habitats in Pocono Creek. Projected increase in the imperviousness in the watershed, on the other hand, is expected to increase flood frequency and reduce the recurrence interval of high flows.

Upon request by the DRBC and the EPA Region III, the National Risk Management Research Laboratory of the USEPA has been tasked to investigate through a watershed model study the impact of projected land use changes on potential alterations in the hydrology of Pocono Creek. Constrained by the existing budget and available resources, it was concluded that the SWAT model is a suitable and effective tool to conduct this modeling study.

The objectives of the watershed model study are primarily three-fold. First, to calibrate and validate a watershed model for Pocono Creek and compute the spatial groundwater recharge distribution for use by a USGS groundwater flow model (MODFLOW) being developed to assess the impact of land-use changes on base flow. Secondly, to compute monthly median daily flows for use by the PIFM model that will be used to establish a relationship between flow reductions and potential habitat degradation in Pocono Creek. Thirdly, to investigate the impact of land-use changes on flow duration characteristics and identify critical areas in the watershed. An important component of this study is investigating NEXRAD as an alternative source of precipitation data, and the error propagation analysis required to examine model forecast quality.

# 2 Model Selection

## 2.1 Background

The distributed hydrologic Soil Water Assessment Tool (SWAT) (Neitsch et al., 2002a/b) was chosen to fulfill the project objectives. The SWAT model was originally developed to quantify the impact of land management practices in large, complex watersheds with varying soils, land use, and management conditions over a long period of time, on the order of years. It is developed and maintained by the US Department of Agriculture (USDA) scientists and is freely available from <http://www.brc.tamus.edu/swat>. Although SWAT is mostly based on empirical equations and simplified mass balance relationships, it is a widely-used model and numerous applications can be found in the peer reviewed literature. For instance, as of February 2006, the SWAT model web site cited 211 peer reviewed publications in the form of journal papers or book chapters (<http://www.brc.tamus.edu/swat/swat-peer-reviewed.pdf>). Borah (2002) reviewed eleven continuous-simulation and single-event watershed scale models including SWAT. The study provides a better understanding of the mathematical bases of the models. Kalin and Hantush (2003) reviewed key features and capabilities of widely cited watershed scale hydrologic and water quality models, and identified SWAT as one of the most suitable models for applications related to watershed management. Robustness of SWAT for simulating watershed responses has also been demonstrated in comparative studies by Saleh and Du (2002) and Van Liew et al. (2003). Arnold and Fohrer (2005) provided a list of SWAT applications in the USA and worldwide.

The SWAT model development, operation, limitations, and assumptions were discussed by Arnold et al. (1998). Srinivasan et al. (1998) reviewed the applications of the SWAT model in streamflow prediction, sediment and nutrients transport, and effects of management practices on water quality. Arnold and Allen (1996) evaluated the performance of different hydrologic components of the SWAT model for three watersheds in Illinois (100-250 $km^2$). Comparing the model outputs to measured data, the calibrated model reasonably simulated runoff, groundwater, and other components of hydrologic cycle for the study watersheds. Most of the simulated average monthly outputs were within 5% of the historical data and nearly all of them were within 25%. The coefficient of determination ($R^2$) was used to assess the correlation between the observed and simulated average monthly variables. Also, the interaction among various components of hydrologic budgets was recognized to be realistic. SWAT was utilized in a study by Arnold et al. (2000) to compare the performance of two baseflow and groundwater recharge models. The first model was the water balance components of the SWAT model. A combination of a digital hydrograph separation tool and a modified hydrograph recession curve displacement technique composed the second model. The results of the two models were in general agreement in the Upper Mississippi river basin. A detailed procedure for calibration of SWAT was laid out by Santhi et al. (2001). Jha et al. (2003) found curve number (CN) as the most sensitive parameter in streamflow prediction with SWAT. Muleta and Nicklow (2005) applied SWAT coupled with automated calibration to estimate daily flow and sediment yield in a 133 $km^2$ Southern Illinois watershed. Eckhardt and Arnold (2001) developed a version of SWAT having global optimization algorithm (SWAT-G) to model daily flow in an 81 $km^2$ watershed in Germany. Fohrer et al. (2002) used SWAT-G in conjunction with two other GIS based agricultural economy and ecology

models in a mountainous 60 $km^2$ watershed in Germany to analyze the effect of land use changes. Sophocleaous and Perkins (2000) integrated SWAT with MODFLOW and applied the integrated modeling system to three different Kansas watersheds. Tripathi et al. (2004) showed on a 92.5 $km^2$ Indian watershed that SWAT can successfully simulate average annual and monthly flow and sediment yield even if weather input is obtained through SWAT's weather generator. One may also refer to Jayakrishnan et al. (2005) on SWAT applications to water resources management. In conclusion, SWAT performance has been extensively validated for streamflow, and sediment and nutrients yield predictions for different regions of United States and outside.

## 2.2 Summary of Hydrologic Component of SWAT Model

SWAT is a distributed, deterministic process-based hydrologic model (Neitsch et al., 2002a/b). The AVSWAT (Di Luzio et al., 2002) graphical user interface (GUI) which runs under ArcView GIS is used to preprocess model data, run the SWAT model, and post process model outputs. SWAT uses readily available inputs and has the capability of routing runoff and chemicals through streams and reservoirs, adding flows and input measured data from point sources, and is capable of simulating long periods for computing the effect of management changes. Major components of the model include weather, surface runoff, return flow, percolation, evapotranspiration (ET), transmission losses, pond & reservoir storage, crop growth & irrigation, groundwater flow, reach routing, nutrient & pesticide loading, and water transfer.

Input data needed to run the SWAT model includes soil, land use, weather, rainfall, management conditions, stream network, and watershed configuration data. AVSWAT has the capability of extracting most of these model parameters from readily available GIS maps such as digital elevation models (DEM), land use maps, STATSGO soil maps, etc. Below is a short summary of the SWAT model from the model manual and theoretical documentation version 2000 (Neitsch et al., 2002a; 2002b).

SWAT partitions the watershed into subunits including subbasins, reach/main channel segments, impoundments on main channel network, and point sources to set up a watershed. Subbasins are divided into hydrologic response units (HRUs) which are portions of subbasins with unique land use/management/soil attributes. AVSWAT enables extraction of input parameters easily. It uses Digital Elevation Models (DEM) as input to extract the channel network and delineate the watershed and subwatersheds, the resolution of which depends on the user provided threshold area which is required to initiate a first order channel. The threshold area can be chosen in such a way that the resultant channel network resembles the one provided in topographic maps. The user needs to provide two threshold values to create HRUs, one for land use and one for soil. Land uses that cover a percentage of the subbasin area less than the threshold level are considered minor and thus eliminated. After the elimination process, the areas of the remaining land uses are reapportioned so that 100% of the land area in the subbasin is modeled. The soil threshold is applied next in a similar fashion to eliminate minor soil types that occupy negligible portions of the HRUs.

In SWAT, the land phase of the hydrologic cycle is based on the water balance equation:

$$SW_t = SW_0 + \sum_{i=1}^{t}(R_{day,i} - Q_{surf,i} - E_{a,i} - w_{seep,i} - Q_{gw,i}) \quad (2.1)$$

where $SW_t$ is the final soil water content (mm), $SW_0$ is the initial soil water content (mm), $t$ is the time (days), $R_{day,i}$ is the amount of precipitation on day $i$ (mm), $Q_{surf,i}$ is the amount of surface runoff on day $i$ (mm), $E_{a,i}$ is the amount of evapotranspiration on day $i$ (mm), $w_{seep,i}$ is the amount of percolation and bypass flow exiting the soil profile bottom on day $i$ (mm), and $Q_{gw,i}$ is the amount of return flow on day $i$ (mm).

Snowmelt is included with rainfall in the calculation of runoff and percolation; it is controlled by the air and snow pack temperature, the melting rate, and the areal coverage of snow. The mass balance for the snow pack is given by:

$$SNO_t = SNO_0 + R_{day} - E_{sub} - SNO_{mlt} \quad (2.2)$$

where $SNO_t$ is the water content of the snow pack at the end of a day (mm), $SNO_0$ is the initial water content of snow pack (mm), $R_{day}$ is the amount of precipitation on a given day (mm), $E_{sub}$ is the amount of sublimation on a given day (mm), and $SNO_{mlt}$ is the amount of snowmelt on a given day (mm). This equation assumes that the water released from snowmelt is evenly distributed over the 24 hours of the day.

SWAT uses the SCS curve number method (USDA Soil Conservation Service, 1972) or Green & Ampt infiltration method (Green and Ampt, 1911) to compute surface runoff volume for each HRU. The former option is utilized in this study. The SCS runoff equation is an empirical model that was developed to provide a consistent basis for estimating the amounts of runoff under varying land use, soil types, and antecedent moisture conditions (Rallison and Miller, 1981). The SCS curve number equation is:

$$Q_{surf} = \frac{(R_{day} - 0.2S)^2}{(R_{day} + 0.8S)} \quad (2.3)$$

where, $S$ is the retention parameter (mm). In this equation the initial abstraction, which includes surface storage, interception and infiltration prior to runoff, is approximated as $0.2S$. The retention parameter is defined as:

$$S = 25.4\left(\frac{1000}{CN} - 10\right) \quad (2.4)$$

in which $CN$ is the curve number for the day, which is a function of the soil's permeability, land use and antecedent soil water conditions.

Evapotranspiration (ET) is the primary mechanism by which the water is removed from a watershed. It includes all processes by which water at the earth's surface is converted to water vapor: evaporation from the plant canopy, transpiration, sublimation and evaporation from the soil. SWAT calculates actual ET from potential evapotranspiration (PET). The latter is estimated by three methods in SWAT: the Penman-Monteith method, the Priestly-Taylor method, and the Hargreaves method. The Penman-Monteith method requires solar radiation, air temperature, relative humidity and wind speed. The Priestly-Taylor method requires solar radiation, air temperature and relative humidity. The Hargreaves method requires air temperature only. Penman-Monteith is used in this study.

Once surface runoff is calculated, the amount of surface runoff released to the main channel is computed from

$$Q_{ch,i} = \left(Q_{surf,i} + Q_{stor,i-1}\right) \cdot \left[1 - e^{\frac{-surlag}{t_{conc}}}\right] \tag{2.5}$$

where $Q_{ch,i}$ is the amount of surface runoff discharged to the main channel on day $i$ (mm), $Q_{surf,i}$ is the amount of surface runoff generated in the subbasin on day $i$ (mm), $Q_{stor,i\text{-}1}$ is the surface runoff stored or lagged from day $i$-1 (mm), *surlag* is the surface runoff lag coefficient, and $t_{conc}$ is the time of concentration for the subbasin (hrs). The last expression within the bracket on the right hand side of Equation (2.5) represents the fraction of total available water allowed to enter the reach on a given day. Remaining water becomes available water for the next day ($Q_{stor,i}$).

The movement of water through the channel network of the watershed to the outlet is routed in main channel and reservoirs. Flow is routed through the channel using a variable storage coefficient method developed by Williams (1969) or the Muskingum routing method, the latter of which is employed in this study. Transmission losses, which reduce runoff volume as the flood wave travels downstream, are also accounted for by the model. SWAT is a continuous time model, i.e., a long-term yield model. The model is not designed to simulate detailed, single-event flood routing.

The water balance for the shallow aquifer is:

$$aq_{sh,i} = aq_{sh,i-1} + w_{rchrg,i} - Q_{gw,i} - w_{revap,i} - w_{deep,i} - w_{pump,sh,i} \tag{2.6}$$

in which $aq_{sh,i}$ is the amount of water stored in the shallow aquifer on day $i$ (mm), $aq_{sh,i\text{-}1}$ is the amount of water stored in the shallow aquifer on day $i$-1 (mm), $w_{rchrg,i}$ is the amount of recharge entering the aquifer on day $i$ (mm), $Q_{gw,i}$ is the groundwater discharge, or base flow, into the main channel on day $i$ (mm), $w_{revap,i}$ is the amount of water moving into the soil zone in response to water deficiencies on day $i$ (mm), $w_{deep,i}$ is the amount of water percolating from the shallow aquifer into the deep aquifer on day $i$ (mm), and $w_{pump,sh,i}$ is the amount of water removed from the shallow aquifer by pumping on day $i$ (mm). The recharge to the aquifer on a given day is calculated:

$$w_{rchrg,i} = \left[1 - e^{-1/\delta_{gw}}\right] \cdot w_{seep,i} + e^{-1/\delta_{gw}} \cdot w_{rchrg,i-1} \tag{2.7}$$

where $\delta_{gw}$ is the delay time or drainage time of the overlying geologic formations (days), $w_{seep,i}$ is the total amount of water exiting the bottom of the soil profile on day $i$ (mm), and $w_{rchg,i\text{-}1}$ is the amount of recharge entering the aquifer on day $i$-1 (mm).

Base flow is computed by SWAT using this equation:

$$Q_{gw,i} = e^{-\alpha_{gw}\Delta t} \cdot Q_{gw,i-1} + \left(1 - e^{-\alpha_{gw}\Delta t}\right) \cdot w_{rchrg,i} \tag{2.8}$$

where $Q_{gw,i\text{-}1}$ is the groundwater flow into the main channel on day $i$-1 (mm), $\alpha_{gw}$ is the base flow recession constant, and $\Delta t$ is the time step (1 day).

## 2.3 Summary

The rationale for the selection of SWAT was laid down in this section and its track record of applications to watershed management was discussed. It should be noted that while it is not the policy of the U.S. EPA to promote the use of a particular model, the unavailability of a detailed survey of Pocono Creek channels' geometry and characteristics and lack of information about bathymetric and hydraulic characteristics of impoundments, ponds, and wetlands in the watershed precluded the use of more physically based, complex watershed models that are currently available to the public. It will be evident throughout the analyses hereafter that the selection of the SWAT model was indeed an appropriate decision.

SWAT is a distributed, process-based watershed model, but with significant number of empirical relationships. It is one of the most suitable models for assessing the impact of management practices and land disturbances on watershed responses, and has a solid track record of applications.

# 3 Watershed Model

## 3.1 Study Area

The 120 $km^2$ Pocono Creek watershed is located between the latitudes $40^0$59'N-$41^0$06'N and longitudes $75^0$14'W-$75^0$26'W in Monroe County, Eastern Pennsylvania near the New Jersey state border (Figure 1), located within the Delaware River Basin. Pocono Creek's 26 km long watershed valley drains from the Pocono Plateau in its headwaters eventually into the Brodhead Creek, a tributary to the Delaware River. The model is constructed for the area upstream from the USGS streamflow gauge station that is located about 6.4 km upstream from the mouth near the city of Stroudsburg, PA (Figure 1) and drains an area about 98.87 $km^2$.

Table 1 summarizes the data used in this study along with their sources and formats. Precipitation, temperature, humidity and wind speed data were obtained from two National Weather Service (NWS) climate stations; Mount Pocono to the North and Stroudsburg to the East. As can be seen from Figure 1, both stations are outside the watershed boundary. To study the potential effects of this on model performance, NEXRAD data were also utilized during the study as an alternative precipitation data source. Specifically, the XMRG products produced by The Middle Atlantic River Forecast Center (MARFC - <http://www.erh.noaa.gov/er/marfc>) were used. XMRG precipitation files are generated in a specific file format after analyses from both gauges and radar with some manual quality control and are available at approximately 4 km cell resolutions. The small squares with dots inside in Figure 1 represent the locations of the centroids of the NEXRAD precipitation cells. The XMRG files for the MARFC region can be downloaded from <http://dipper.nws.noaa.gov/hdsb/data/nexrad/marfc_mpe.php>. Climate data from 1960 to 2004 indicate that, on average, annual precipitation is 1237 mm, and varies from a minimum of 76 mm in February to a maximum of 125 mm in September. The temperature typically varies from a minimum of -11 $^oC$ in January to a maximum of 26 $^oC$ in July.

The current land cover (Figure 2a) is dominantly forest (89%). Pasture constitutes about 3.5% and minor agricultural activities less than 0.2%. Residential, commercial and transportation areas comprise about 5.8% of the watershed including the commercially developed Route 611 corridor, Big Pocono State Park, Camelback Ski Area, the Nature Conservancy's Tannersville Cranberry Bog, and state gamelands. Silt loam is the major soil type in the watershed covering about 84.9%. Two other soil types in the watershed are sandy loam (11.4%) and loam (3.7%). The elevation in the watershed changes from 183 m at the outlet to 648 m near the Camel Back Ski Area. The topography in the watershed generally has an average slope of 11% and ranges from 4% to 23%. A 30 m resolution digital elevation model (DEM) is used in extraction of the stream network and delineation of the watershed and subwatersheds. The watershed is divided into 29 subbasins. The STATSGO soil database was used to acquire the soil-related model parameters (Figure 2b). Hydrologic response units (HRU) are generated by using 10% and 0% thresholds for land use and soil maps that resulted in a total of 129 HRUs.

Table 1. Data used in the model construct and their sources.

| Data | Source | Additional Info |
|---|---|---|
| Soil | SWAT build in | USDA STATSGO soil database |
| Land Use | DRBC | National Land Cover Data (NLCD) |
| Elevation | DRBC provided, also available at http://www.pasda.psu.edu/ | 30 m resolution DEM |
| Climate | NOAA National Data Center http://nndc.noaa.gov | Stations: Mount Pocono, 41°08'N / 75°23'W; Stroudsburg, 41°01'N / 75°11'W; hourly (daily for Stroudsburg) precipitation, temperature, wind speed, relative humidity |
| Radar | NWS Hydrologic Data Systems Group: http://dipper.nws.noaa.gov/hdsb/data/nexrad/nexrad.html | NEXRAD, Multisensor Precipitation Estimator (MPE) Data in XMRG format. Hourly precipitation at approximately 4 km resolution. |
| Stream flow | http://waterdata.usgs.gov/pa/nwis/uv?dd_cd=02&format=pre&period=16&site_no=01441495 | USGS 01441495 Pocono Creek ab Wigwam Run near Stroudsburg, PA, Lat $40^0$59'27", long $75^0$15'20", data collected every 15 min. |

### 3.2 Base flow Separation

Stream flow is usually partitioned into two parts: the fast and the slow response components, the latter of which is due to the base flow contribution. Any other contribution to stream flow by various mechanisms can be deemed as the fast response component. SWAT computes the base flow and surface runoff components of the stream flow separately. Although some parameters play an interactive role such as the CN, some parameters only affect one individual component of the flow. For instance, Manning's roughness only affects surface runoff, whereas base flow recession constant only affects base flow. Hence, to better calibrate model parameters it is necessary to partition the observed stream flow hydrograph into base flow and surface runoff components, both of which then become estimated quantities rather than observed.

We estimated base flow using the method described in Arnold et al. (1995) and Arnold and Allen (1999). This is a recursive digital filter technique which was originally used in signal processing and filtering. The filter can be passed over the stream flow data several times with each pass resulting in less base flow. Various other methods of base flow separation are also available and each can give significantly different base-flow estimates which clearly affect not only model calibrated parameters but also model performance.

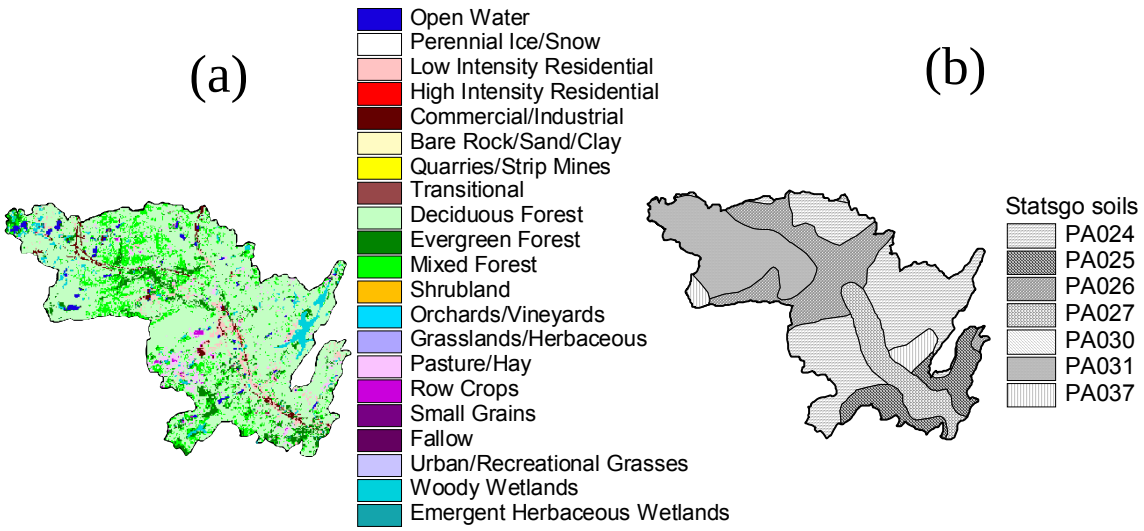


Figure 2. Pocono Creek watershed: a) Land use map; b) Soil map (STATSGO).

### 3.3 Next Generation Weather Radar (NEXRAD)

Both the Mount Pocono and Stroudsburg climate stations are located outside the watershed boundary (Figure 1) and provide point measurements. This raises the question whether the data from these two gauge stations are representative of spatial rainfall pattern over the Pocono Creek watershed which is partly covered with mountains. It is well known that precipitation may change significantly in mountainous areas due to orographic effects. Precipitation is usually higher in upper elevations. To be able to realistically answer this question several raingauges inside the watershed boundary are needed so that spatial distribution of the precipitation pattern can be attained. The Next Generation Weather Radar (NEXRAD) precipitation data offer an opportunity to overlay spatially distributed precipitation over the entire watershed. NEXRAD also provides a finer temporal resolution (hourly) compared to daily values from the climate stations that are available. In any case, hourly precipitation is not required for this study and daily precipitation suffices for the current model application. Because the ultimate goal is modeling base flow and stream flow in the Pocono Creek watershed, gauge driven model performance is compared to NEXRAD driven ones. This sheds light on whether or not consideration of the distributed nature of precipitation improves the model performance, and whether NEXRAD can be relied on as an alternative to the surface raingauge measurements. For further details on processing the NEXRAD data for use in a watershed model, the reader may refer to Kalin and Hantush (2006a).

### 3.4 Model Calibration

Models are only simplified representations of natural processes. Even fully physically-based models cannot avoid simplifications. In addition, parametric uncertainty and measurement errors make model calibration inevitable in most modeling exercises. A split data set approach is implemented in this study to calibrate and validate the SWAT model. The period

from 7/1/02 to 5/31/04 of the daily flow data, aggregated into monthly flows, is used for calibration and the remaining data from 6/1/04 to 4/30/05 is used for validation. Three to five years of data are typically required in calibration, although along with a good set of data and proper objective function, a single year of data has been shown to be adequate (Sorooshian et al., 1983). The statistical measures of Mass Balance Error (*MBE*), coefficient of determination ($R^2$) and Nash-Sutcliffe (1970) efficiency ($E_{NS}$) are used as indicators of model performance that are defined as

$$MBE = \frac{\sum_{i=1}^{N} Q_{sim,i} - \sum_{i=1}^{N} Q_{obs,i}}{\sum_{i=1}^{N} Q_{obs,i}} = \frac{\overline{Q}_{sim} - \overline{Q}_{obs}}{\overline{Q}_{obs}} \tag{3.1}$$

$$R^2 = \frac{\left[\sum_{i=1}^{N} (O_{obs,i} - \overline{O}_{obs})(O_{sim,i} - \overline{O}_{sim})\right]^2}{\left[\sum_{i=1}^{N} (O_{obs,i} - \overline{O}_{obs})^2\right]\left[\sum_{i=1}^{N} (O_{sim,i} - \overline{O}_{sim})^2\right]} \tag{3.2}$$

$$E_{NS} = 1.0 - \frac{\left[\sum_{i=1}^{N} (O_{sim,i} - O_{obs,i})^2\right]}{\left[\sum_{i=1}^{N} (O_{obs,i} - \overline{O}_{obs})^2\right]} \tag{3.3}$$

where $Q_{sim,i}$ and $Q_{obs,i}$ are simulated and observed or estimated flows at $i^{th}$ observation, respectively, $N$ is the number of observations. Similarly, $\overline{O}_{sim}$ and $\overline{O}_{obs}$ are the average simulated and observed flows over the simulation period. The coefficient of determination describes the proportion of the total variances in the observed data that can be explained by the model and ranges from 0 to 1, whereas Nash-Sutcliffe efficiency is a measure of how well the plot of observed versus predicted values fit the 1:1 line, and can vary from $-\infty$ to 1. A negative $E_{NS}$ indicates that model predictions are not better than the average of observed data.

The calibration process is adapted from Santhi et al. (2001) and is summarized in Figure 3. The threshold values set for *MBE*, $R^2$ and $E_{NS}$ in the figure are at monthly time scales. Curve numbers (*CN*) of each soil/land use combination are calibrated first to meet the criteria set for surface runoff (SR). At the next stage the *GW_REVAP* coefficient which is a limiting factor for the maximum amount of water that can be removed from the aquifer to the overlying unsaturated zone due to moisture deficit, threshold depth of water in shallow aquifer required for base flow to occur (*GWQMN*), delay time for aquifer recharge (GW_DELAY), and soil evaporation compensation factor (*ESCO*) are calibrated to meet the stream flow (SF) and base flow (BF) criteria. Once the model is calibrated using measured stream flows for the calibration period, the model is validated using the data for the above stated validation period and *MBE*, $R^2$ and $E_{NS}$ are checked against the threshold values shown in Figure 3. The threshold values set for *MBE*, $R^2$ and $E_{NS}$ statistical measures must be

satisfied for a successfully calibrated model. Before calibrating the model parameters, an automated sensitivity analysis was performed with a version of SWAT called AVSWATX that is based on Latin Hypercube (LH) and One factor At a Time (OAT) sampling. The sensitivity analysis revealed that *CN* is the most sensitive model parameter (Kalin and Hantush, 2006a).

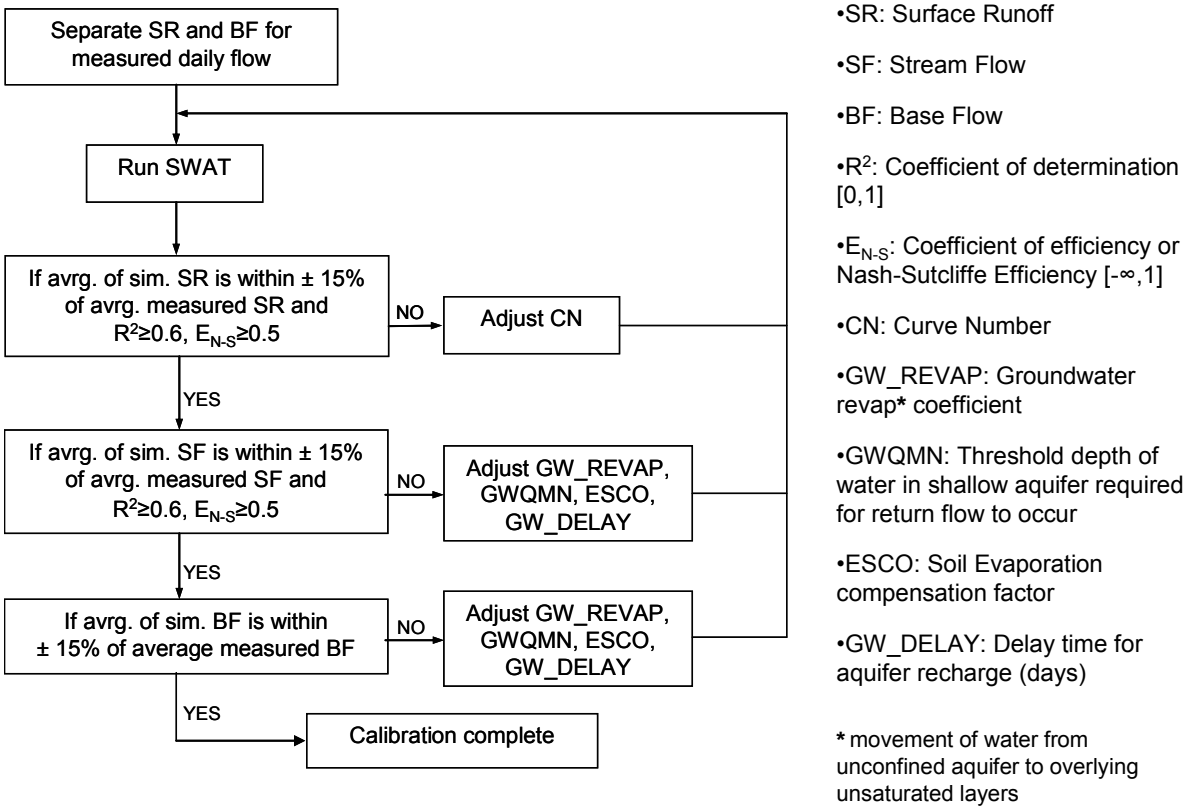


Figure 3. Calibration procedure in the SWAT model (adapted from Santhi et al., 2001).

Figure 4 compares the daily and monthly areally averaged NEXRAD estimated precipitation to measurements at the gauges. All the values in the figure are in mm. Mount Pocono station falls in between two NEXRAD cells (Figure 1): (961,614) and (961,615) where the numbers in parentheses represent the X and Y coordinates of the centroids of NEXRAD cells in the HRAP coordinate system. Therefore, we compared Mount Pocono point precipitation measurements to NEXRAD estimates at both cells as well as to their arithmetic averages. The Stroudsburg station falls inside the grid (966,614) as seen in Figure 1. Estimated hourly precipitations were

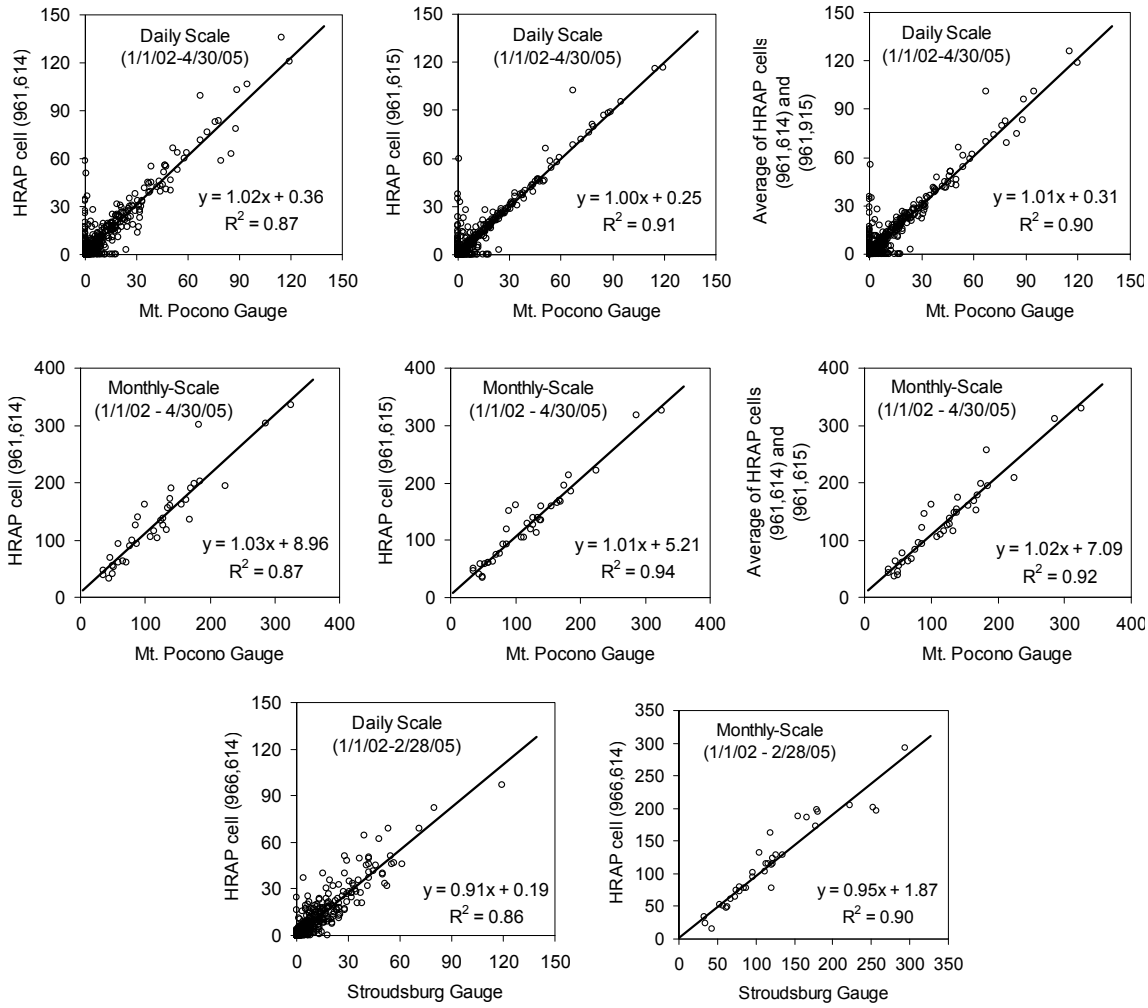


Figure 4. Comparison of NEXRAD estimated precipitation with measurements from local gauge stations. Values shown are in mm.

aggregated in these cells to obtain the daily and monthly precipitation estimates. We computed daily values from 7:00 AM to 7:00 AM at the cell (966,614) to be consistent with the reported daily precipitation data at the Stroudsburg gauge station. Figure 4 reveals that (961,615) represents Mount Pocono relatively better than both (961,614) and the average of the two, as it has a higher $R^2$, the slope of its regression equation is closer to 1 and has a smaller intercept. Further, (961,615) overestimates precipitation by only 5.7% compared to 10.8% overestimation of (961,614) from 1/1/2002 to 4/30/2005. Over the time period from 1/1/2002 to 2/28/2005, NEXRAD underestimates precipitation in the Stroudsburg station by 10.0%. In this watershed, comparisons with gauge measurements indicate that NEXRAD technology provides an alternative source of precipitation data. Note that NEXRAD estimates are areal average precipitations of an approximately 4x4 $km^2$ grid in contrast to point measurements (~100 $cm^2$) of gauge stations. Differences between the two are partly attributed to variations of point measurements from areal average estimates of precipitations, and partly due to measurement errors associated with the instrument itself.

SWAT is calibrated both with rain gauge and NEXRAD as the precipitation data source. The simulations are performed starting from 7/1/1970, i.e., with a 32 years of warm up period to minimize the effect of initial conditions. For more details on calibration using raingauge data, the readers are referred to Kalin and Hantush (2006a). The surface runoff lag coefficient (*surlag*) had to be adjusted to improve the daily simulation performances. The *CN* values calibrated based on raingauge data are reduced in all HRUs by 1.5 (for this specific site) when NEXRAD was the data source. The volume of precipitation over the study watershed estimated with NEXRAD is greater than that estimated from raingauges, and thus this adjustment in *CN* had to be made. Experimentation with other parameters revealed no further improvement in the model performance. Figure 5 compares SWAT simulations to observed SF and estimated SR at the monthly time scale and SF at the daily time scale only for NEXRAD. Rain gauge simulations not shown on the figure as hydrographs are very similar to NEXRAD generated hydrographs.

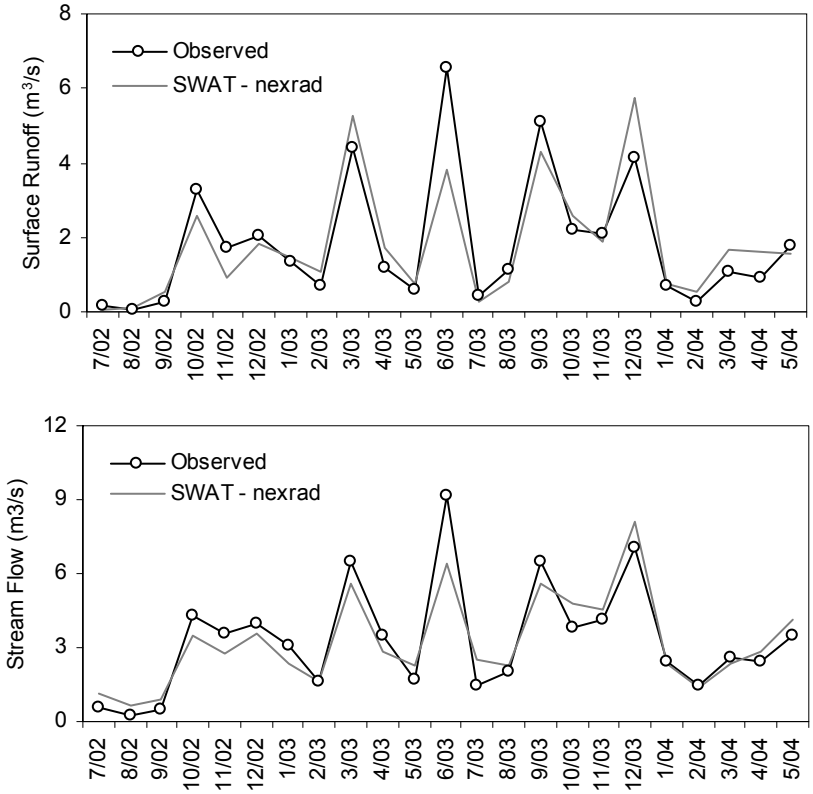

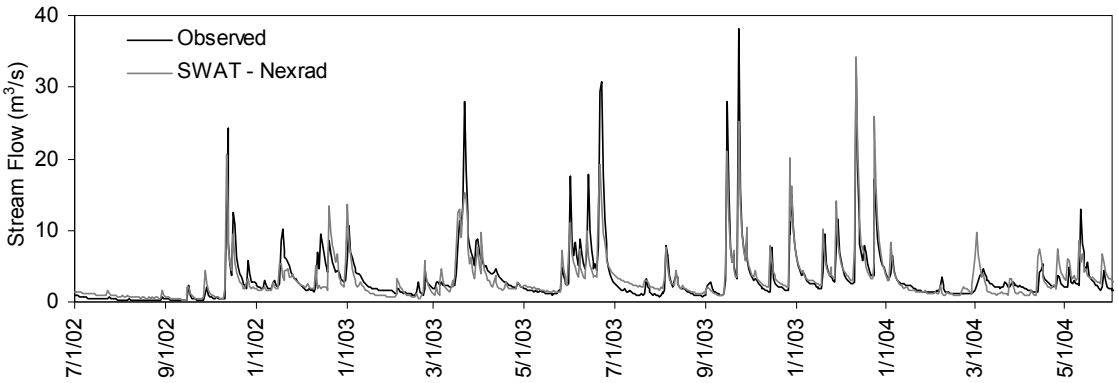


Figure 5. Measured stream flow (SF) and estimated surface runoff (SR) plotted against SWAT simulated counterparts for the calibration (7/1/2002-5/31/2004) period. NEXRAD estimates are used as precipitation data source. Top two panels show monthly results, and the bottom panel shows daily results.

As Figure 5 shows, overall the model performs well at both time scales. These results are comparable to gauge driven simulations (Kalin and Hantush, 2006a). The NEXRAD driven model performance statistics *MBE*, $R^2$ and $E_{NS}$ are summarized in Table 2 and are well within the calibration threshold values shown in Figure 3. From the results obtained, although with a relatively smaller calibrated *CN*, it is reasonable to conclude that NEXRAD estimated precipitation data is a good alternative to gauge measured precipitation data. The benefit of using distributed rainfall data was negligible at both time scales for the particular application. On the other hand, noticeable improvement is expected for stream flow estimates at the interior subwatershed outlets with the use of distributed rainfall data over the available raingauge data. In the next section, an 11 month period split sample data set is used to validate the calibrated model.

Table 2. Mass Balance Error (*MBE*), coefficient of determination, $R^2$, and Nash-Sutcliffe efficiency, $E_{NS}$ for Stream Flow (SF), Base flow (BF) and Surface Runoff (SR) during the calibration period with NEXRAD as precipitation data source. Values in parenthesis indicate values when rain gauges are used as precipitation data source.

| | Stream Flow (SF) | | | Base Flow (BF) | | | Surface Runoff (SR) | | |
|---|---|---|---|---|---|---|---|---|---|
| | *MBE* (%) | $R^2$ | $E_{NS}$ | *MBE* % | $R^2$ | $E_{NS}$ | *MBE* % | $R^2$ | $E_{NS}$ |
| Monthly | -3.8 | 0.85 | 0.84 | -4.5 | 0.31 | 0.05 | -3.2 | 0.79 | 0.79 |
| | (-3.8) | (0.85) | (0.83) | (-4.0) | (0.30) | (0.08) | (-3.6) | (0.77) | (0.77) |
| Daily | | 0.74 | 0.73 | | | | | | |
| | | (0.74) | (0.74) | | | | | | |

### 3.5 Model Validation

The period from 6/1/2004 to 4/30/2005 is chosen as the validation period. Simulations are performed again starting from 7/1/1970 to curtail the effect of initial conditions. Figure 6 compares observed values to model simulations conducted with NEXRAD data. In the figure the top two panels compare monthly SF and SR and the bottom figure is for daily SF results. From visual inspection, one can conclude that model simulations match well with observed SF and estimated SR.

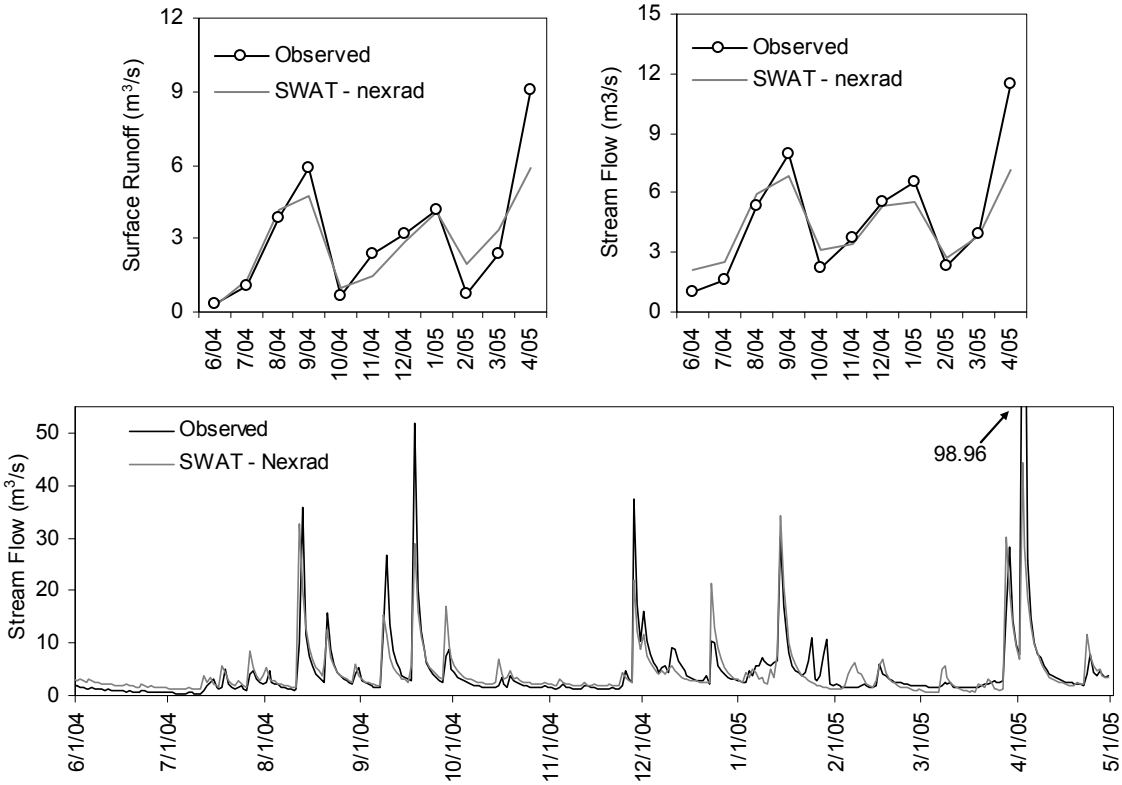


Figure 6. Measured streamflow (SF) and estimated surface runoff (SR) plotted against SWAT simulated counterparts for the validation period (6/1/2004-4/30/2005). NEXRAD estimates are used as precipitation data source. Top and bottom panels denote monthly and daily results, respectively.

Table 3 summarizes the model efficiencies at the monthly and daily time scales, respectively, validated with NEXRAD and raingauge data. In the table "g" denotes gauge input and "n" indicates NEXRAD input precipitation. In all cases, the model calibration criteria are satisfied. As can be seen, *MBE* in SR decreased in absolute value from 15.1% to 7.9% with the NEXRAD input simulations. In SF and BF, *MBE* dropped in absolute value to 5.6% from 13.5% and to 1.2% from 10.6%, respectively, all underestimations. Overall NEXRAD input

monthly simulations outperformed raingauge based simulations. Daily statistics showed mixed results.

Table 3. Mass Balance Error (*MBE*), coefficient of determination, $R^2$, and Nash-Sutcliffe efficiency, $E_{NS}$ for Stream Flow (SF), Base flow (BF) and Surface Runoff (SR) during the validation period. g and n represent gauge and NEXRAD input precipitations, respectively.

| | | Stream Flow (SF) | | | Base Flow (BF) | | | Surface Runoff (SR) | | |
|---|---|---|---|---|---|---|---|---|---|---|
| | Precip. source | *MBE* (%) | $R^2$ | $E_{NS}$ | *MBE* % | $R^2$ | $E_{NS}$ | *MBE* % | $R^2$ | $E_{NS}$ |
| Monthly | g | -13.5 | 0.81 | 0.66 | -10.6 | 0.13 | -0.26 | -15.1 | 0.83 | 0.73 |
| | n | -5.6 | 0.89 | 0.75 | -1.2 | 0.06 | -0.40 | -7.9 | 0.84 | 0.77 |
| Daily | g | | 0.70 | 0.64 | | | | | | |
| | n | | 0.66 | 0.62 | | | | | | |

It is interesting to note that while at the monthly time scale NEXRAD had better performance statistics, at the daily time scale gauge driven simulations had slightly better statistics. Several reasons may have contributed to this. First, calibration efforts were more focused to monthly time scale as part of the project goal. Secondly, NEXRAD calibration was built on the calibrated parameters with gauge driven data, therefore there is a small bias.

An additional set of 5 months streamflow data in the period 5/1/2005 to 9/30/2005, which was not available during model validation, was downloaded from the source and was utilized to further evaluate the model performance. The model was run with NEXRAD data and corresponding calibrated parameters during this post-validation period, and the results are plotted in Figure 7. Interestingly, expanding the validation period 6/1/2004 – 4/30/2005 to 9/30/2005 results in slightly improved results; the *MBE* in absolute value decreased from 2.9% to 0.8%, daily $R^2$ increased to 0.68 from 0.66, and daily $E_{NS}$ increased from 0.62 to 0.64.

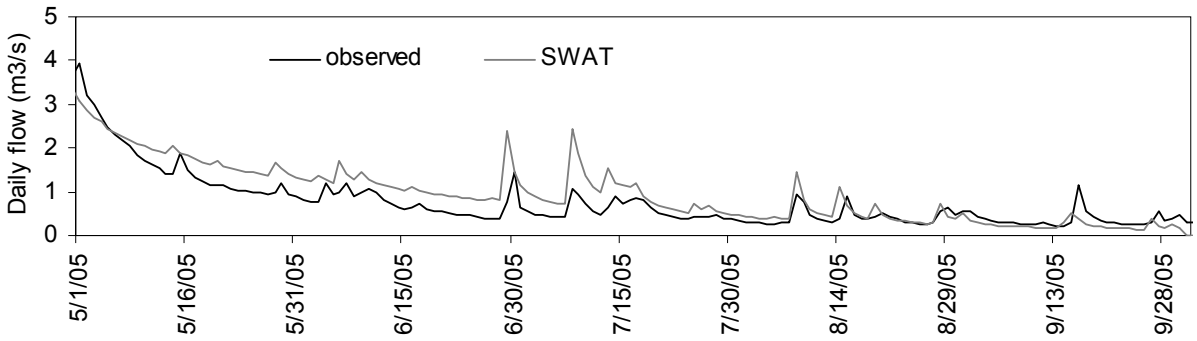


Figure 7. Measured daily streamflows plotted against SWAT simulated counterparts for the post-validation period (5/1/2005-9/30/2005). NEXRAD estimates are used as precipitation data source.

### 3.6 Conclusions

In this section the hydrology in the Pocono Creek watershed was modeled using a distributed parameter watershed model, and in particular the potential for using NEXRAD as an alternative source of precipitation data to raingauge stations was explored. The SWAT model was calibrated and validated for the Pocono Creek watershed.

The model was first calibrated using precipitation data from two gauge stations located outside the watershed boundary. Model performance was evaluated with computed model efficiency statistics, i.e., mass balance error (*MBE*), coefficient of determination ($R^2$), and Nash-Sutcliffe Efficiency ($E_{NS}$). Simulation results were promising at the monthly and daily time scales.

As an alternative data source, the use of radar generated precipitation data (NEXRAD) was appraised. NEXRAD data obtained from the Middle Atlantic River Forecast Center (MARFC) provided hourly precipitation estimates over approximately 4x4 $km^2$ grids. Measured precipitation values at the two gauge stations were in close agreement with the NEXRAD estimated values.

The SWAT model was fed with the spatially distributed NEXRAD precipitation data and recalibrated by reducing the average curve numbers (*CN*) by a value of 1.5 that were obtained from model calibration when gauge precipitation data was used as input. The streamflow and surface runoff hydrographs were in close agreement with measured hydrographs. Efficiency statistics *MBE*, $R^2$ and $E_{NS}$ were close to ones obtained with gauge driven simulations. The model was then run for an additional 11 month period for validation purposes both with gauge and NEXRAD data. NEXRAD generated smaller *MBE*. The values of $R^2$ and $E_{NS}$ were higher at the monthly time scale with NEXRAD, whereas at the daily time scale gauge driven simulations resulted in improved measures of fit. An additional 5 months set of streamflow data was used to further evaluate the performance of the already validated model.

This section showed that spatially distributed precipitation data obtained through radar reflectivity measurements provide a viable alternative to raingauge measurements. However, estimation of precipitation with the help of radar still needs improvements. At present, data from raingauges will continue to be relied upon to correct NEXRAD hourly digital precipitation for mean field bias. Future refinement of this technology may provide a cost-effective alternative source of precipitation data, and may reduce the need for the costlier raingauges for large scale watershed applications.

# 4 Model Prediction Uncertainty

## 4.1 Introduction

It is a common practice that the sequence of sensitivity analysis → calibration → validation is followed during applications of distributed hydrologic/water quality models, yet rigorous attempts are rarely made to assess model predictive uncertainty. Once the model is calibrated with one set of data and validated with another set, it is used for predicting the impact of management practices, land-use changes, and/or long-term climate changes, however, with much less regard to uncertainty bands of predictions. The process of examining model forecast reliability (post-validation) is an important consideration in development of watershed management plans. Modeling uncertainty should be rigorously addressed in development and application of models, especially when the model outcome might have implications on policy, watershed planning and management, and when stakeholders are affected by the decisions contingent upon model-supported analyses (NRC, 2001). Implications of model uncertainty should be factored in the decision making process.

The analysis of uncertainty associated with utility of simulation models appears mostly in the scientific, research literature (e.g., Spear and Hornberger, 1980; Beven and Binely, 1992; Spear et al., 1994; van der Perk and Bierkens, 1997; Saltelli et al., 2000; Hossain et al., 2004; Carpenter and Georgakakos, 2004; and Pebesma et al., 2005). While various approaches exist for estimating distributed watershed/water quality model prediction uncertainty, careful examination of the scientific literature reveals three dominant approaches. Amongst the three approaches, the Bayesian approach is perhaps the most poular. Examples include Bayesian Monte Carlo (e.g., Dilks et al., 1992; and van der Perk and Bierkens, 1997) and Generalized Likelihood Uncertainty Estimation (GLUE) (Beven and Binely, 1992; Freer et al., 1996; Beven and Freer, 2001; Hossain et al., 2004; and Hossain and Anagnostou, 2005) methodologies. A second approach relies directly on Monte Carlo (MC) method to obtain an ensemble of model outputs by independently sampling model parameters from prior distributions based on ranges (i.e., with minima and maxima) derived from literature, or based on new information gained from experience and model calibration (e.g., Binley et al., 1991; Carpenter and Georgakakos, 2004; and Hantush and Kalin, 2005). A third approach can be discerned in which the model noise or residual error is accounted for explicitly (e.g., Sorooshian and Dracup, 1980; and Pebesma et al., 2005). In this approach, model predictions and observations are given as time series data, and attempts are made to fit a deterministic or statistical relationship to the residual time series. Among these three approaches, the third one has been given the least attention. Although GLUE methodology has gained a wider acceptance, the selection of a suitable relationship for computing relative likelihoods associated with the ensemble simulations is a matter of choice, and therefore subjective in that sense. Both the GLUE methodology and the third approach implicitly account for the four major sources of uncertainty: model structural uncertainty, parametric uncertainty, measurement uncertainty, and rainfall variability.

In this section, we fit a time series model to the residuals (observed – predicted) of daily SWAT model output. The focus on model performance at the daily time scale is because

predictions of monthly median daily flows are required inputs to the PIFM model for wild brown trout habitats. The time series model is combined with Monte Carlo-type simulation (Latin Hypercube) to estimate uncertainty bounds for model predictions. Using a new set of streamflow data (i.e., different from calibration and validation data), SWAT model forecast performance is evaluated by comparison of the 90% confidence interval or (uncertainty band) with observed values. One of the advantages of the time series approach, which is described in the following section, is that the commonly adopted Gaussian and statistical independence assumptions for model errors are relaxed by brute force application of time series analysis and using a nonparametric probabilistic approach. Further, MC-type simulation is conducted on rather a simple time series model for the residual errors as opposed to the computationally demanding watershed model.

## 4.2 Structural and Model Parameters Uncertainty

### 4.2.1 Prediction Error

Figure 8(a) shows the time series of model prediction errors (observed-simulated) based on simulations during the calibration and validation period (7/1/2002-4/30/2005). The error is defined by this equation

$$\varepsilon_t = o_t - p_t \tag{4.1}$$

where $\varepsilon_t$ is model output noise or prediction error; $o_t$ is measured streamflow; and $p_t$ is model computed streamflow; and $t$ is time index in days. The $\varepsilon_t$ accounts for model structural uncertainty, parametric uncertainty, measurement uncertainty, and errors in the rainfall input. Model structural uncertainty is usually associated with imperfect knowledge, and generally referred to as epistemic uncertainty. A close look at the daily errors time series (Figure 8a) reveals systematic errors shown as large positive or negative spikes that are not random in nature. In many instances a large (-) error is immediately followed by a big (+) error. One reason might be timing errors in recording either the precipitation or the streamflow. Another, probably the more reasonable, explanation is the inability of the SWAT model to use sub daily rainfall data. When a big rainfall event happens at the very end of a day, the actual watershed response will be about 1 day delayed compared to what SWAT actually simulates with daily rainfall data. This will clearly result in overprediction (negative error) and underprediction (positive error) on two successive days, respectively. Hence, to minimize this type of error to some extent, we decided to use three days (3-day) moving average of the errors in constructing our model. While one may argue as to why daily simulations are of interest, especially when SWAT is best suited for long-term simulations (monthly and annual time steps), there are two compelling reasons for this consideration. First, monthly median daily flows are a required input to the PIFM habitat model. Secondly, there is not sufficient monthly streamflow data to conduct a meaningful time series analysis to model errors. Therefore, in addition to smoothing the effect of the large errors during significant events, a 3-day averaging of streamflows is intended to provide reasonable estimates of daily flows for the wild brown trout habitat model. Further, sufficient data of 3-day moving averages will be available to construct a time series model of residual errors $\varepsilon_t$.

Henceforth, $\varepsilon_t$ refers to model residual errors based on 3-day averages of $o_t$ and $p_t$, and thus deemed (i.e., $\varepsilon_t$) a surrogate to (rather than exact) daily model prediction errors.

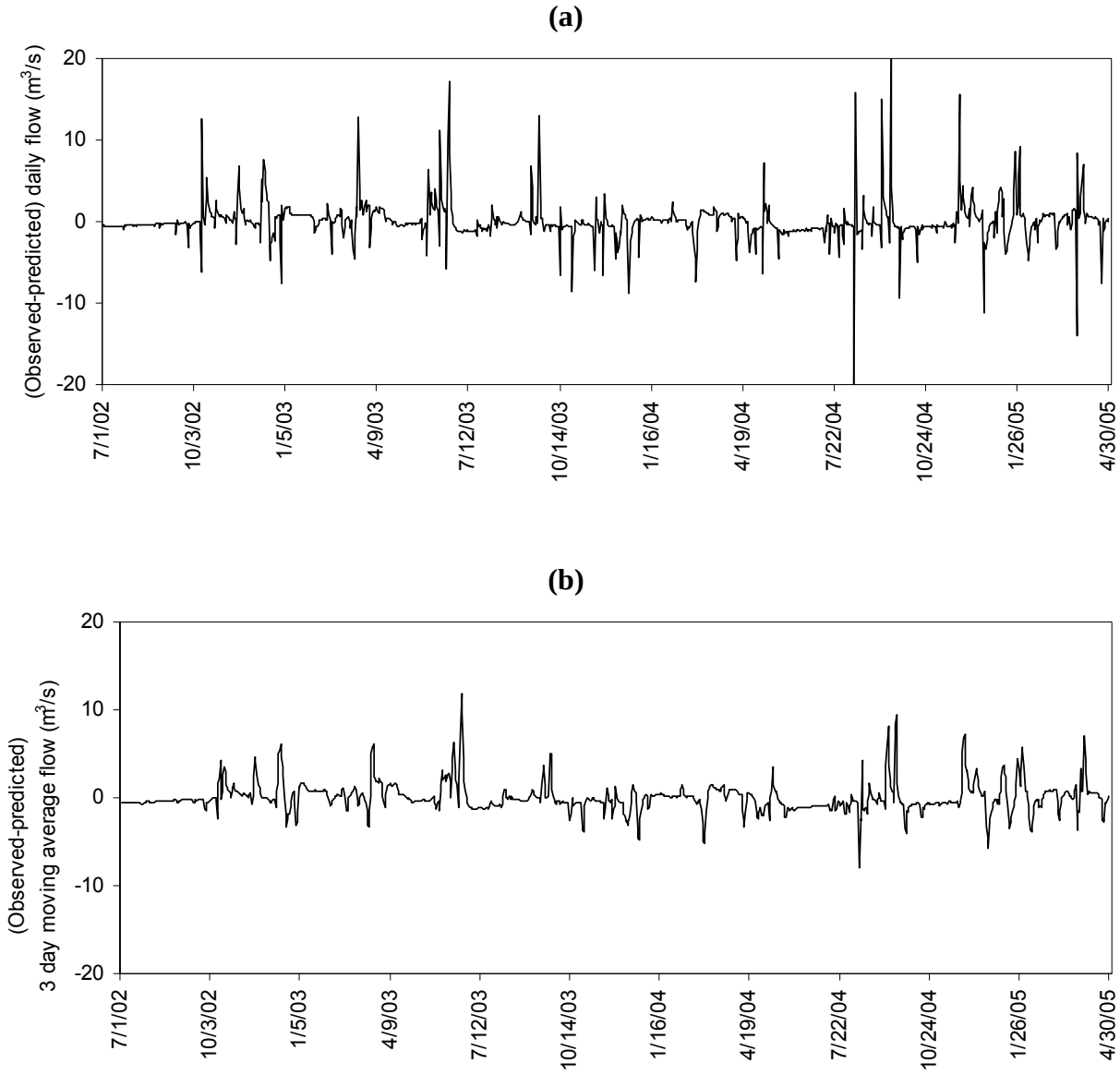


Figure 8. Time series of model prediction errors (Observed – SWAT simulated) in the calibration and validation time period (7/1/2002-4/30/2005): (a) daily simulations, (b) 3-day moving average.

Figure 8(b) shows the difference between 3-day average of observed minus predicted times series of stream flows during the period (7/1/2002-4/30/2005). The errors are not totally eliminated but their magnitudes are significantly reduced. The Minitab® statistical computer package is used to identify a time series model and construct reasonable forecasts for the future of $\varepsilon_t$. In general, a multiplicative seasonal autoregressive integrated moving average model denoted by ARIMA $(p,d,q) \times (P,D,Q)_S$ is fitted to the series of interest, which is the model prediction error $\varepsilon_t$ in our case. The parameters $p$, $d$, and $q$ are, respectively, the

orders of the autoregressive, difference, and moving average operators; $P$, $D$, and $Q$ are, respectively, the orders of the seasonal autoregressive, seasonal moving average, and seasonal difference operators; and $S$ is the seasonal period. Autocorrelation function (ACF) and partial autocorrelation function (PACF) are utilized and the procedure outlined by Shumway (1988), which derive its basis from Box and Jenkins (1970), is followed to identify the best model. The objective of the model identification process is to produce identically distributed, independent residuals $w_t$, with a minimum variance $\sigma_w^2$ arising from fitting some ARIMA $(p,d,q) \times (P,D,Q)_S$ to the $\varepsilon_t$ time series.

The upper two panels in Figure 9 (i.e., Figure 9(a)) show the ACF and PACF of model errors, $\varepsilon_t$. It is obvious that the series display nonstationarity accentuated by the slowly decaying ACF as a function of lag and the large positive value of PACF at lag 1. The ACF of the first difference in Figure 9(b) contains a fairly strong negative peak (-0.44) at lag-3 and zero thereafter, indicating that a seasonal moving average with $S$ = 3 (days) and $Q$ =1 might be appropriate. The decreasing peaks of the PACF at multiples of 3 are due to the seasonal moving average component. Therefore, ARIMA $(0,1,0) \times (0,0,1)_3$ appears to be, at the moment, a suitable selection among, perhaps, other competing models. Table 4 lists several ARIMA models with computed variance of residuals, $\hat{\sigma}_w^2$, and various goodness-of-fit measures: final prediction error (FPF), Akaike's information criterion (AIC), and Bayesian information criterion (BIC). It is clear that the most appropriate model choice is ARIMA $(1,1,1) \times (0,0,1)_3$, which has the smallest values of $\hat{\sigma}_w^2$, FPF, AIC, and BIC. The model was fitted to the error time series depicted in Figure 8(b) (recall the 3-day averages of the actual model errors), and the equation for determining the residuals $w_t$ is

$$(1-\phi B)\nabla \varepsilon_t = (1-\Theta B^3)(1-\theta B) w_t \tag{4.2}$$

where $\nabla \varepsilon_t = \varepsilon_t - \varepsilon_{t-1}$ is the first difference operator; $B\varepsilon_t = \varepsilon_{t-1}$ is the backward shift operator; $\phi$, $\theta$, and $\Theta$ are the fitted parameters. Equation (4.2) can be expanded to yield the following representation for $\varepsilon_t$:

$$\varepsilon_t = (1+\phi)\varepsilon_{t-1} - \phi \varepsilon_{t-2} + w_t - \theta w_{t-1} - \Theta w_{t-3} + \theta \Theta w_{t-4} \tag{4.3}$$

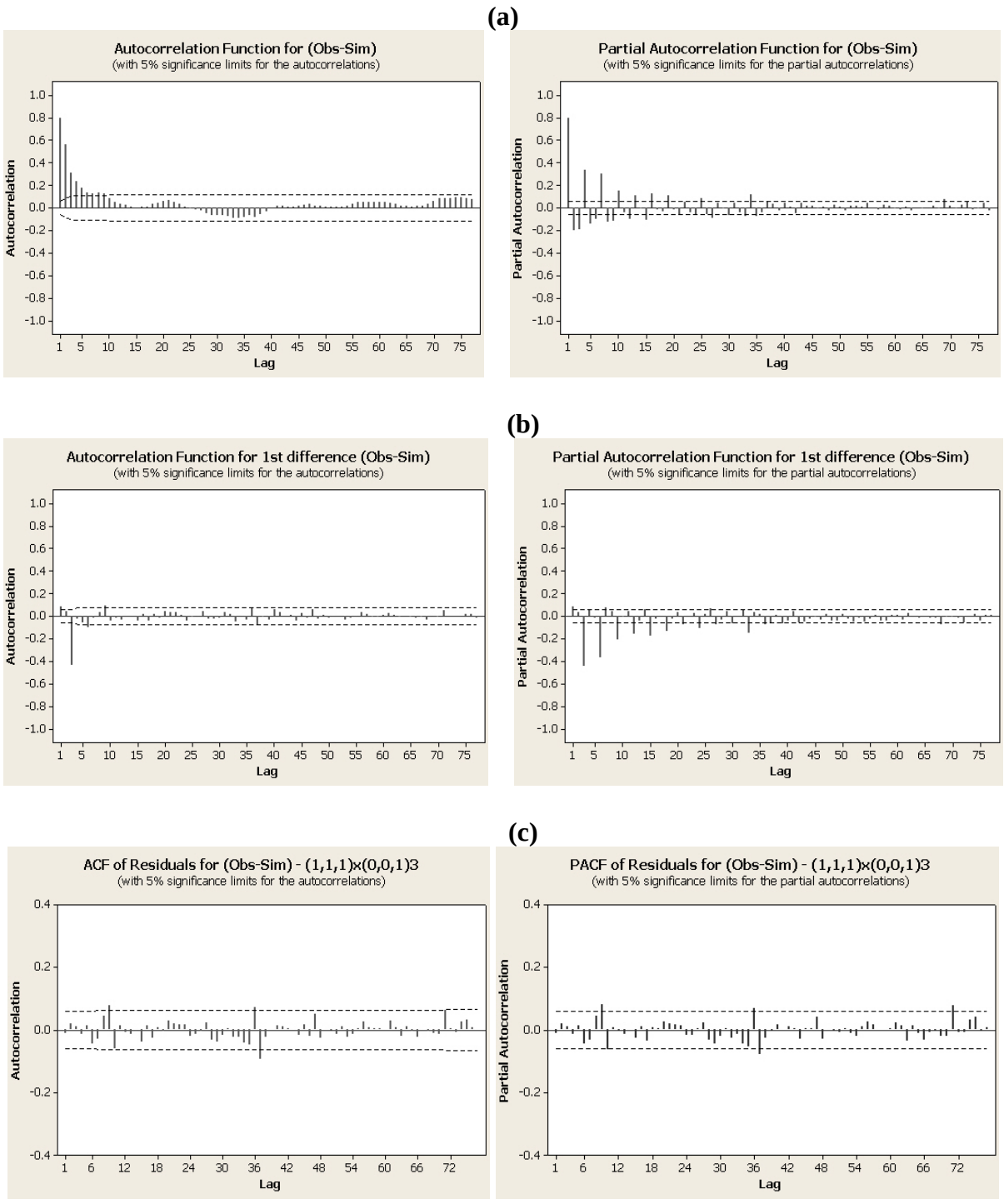


Figure 9. Autocorrelation (ACF) and partial autocorrelation (PACF) functions of: (a) prediction error $\varepsilon_t$, (b) first difference of residual error $\nabla\varepsilon_t = \varepsilon_t - \varepsilon_{t-1}$, (c) residuals ($w_t$) for ARIMA(1,1,1) × $(0,0,1)_3$. The lag is in units of days.

where $\hat{\phi}$ = 0.7838, $\hat{\theta}$ = 0.6163, and $\hat{\Theta}$ = 0.9819. The ACF and PACF of the residuals $w_t$ from this model is plotted in Figure 9(c), and shows no prominent peaks at 5% significance limits. Therefore, it seems reasonable to regard the residuals as being white noise, with an estimated variance $\hat{\sigma}_w^2$ = 0.629.

Table 4. Values of residual variance, Final prediction error (FPF), Akaike's information criterion (AIC), and Bayesian information criterion (BIC) for various models applied to model prediction error data, $\varepsilon_t$.

| Model | $\hat{\sigma}_w^2$ | FPE | AIC | BIC |
|---|---|---|---|---|
| ARIMA(0,1,0)x(1,0,0)$_3$ | 0.926 | 0.928 | -0.075 | -0.070 |
| ARIMA(0,1,0)x(2,0,0)$_3$ | 0.805 | 0.808 | -0.213 | -0.203 |
| ARIMA(0,1,0)x(3,0,0)$_3$ | 0.778 | 0.783 | -0.245 | -0.231 |
| ARIMA(0,1,0)x(4,0,0)$_3$ | 0.762 | 0.768 | -0.264 | -0.245 |
| ARIMA(0,1,0)x(5,0,0)$_3$ | 0.743 | 0.750 | -0.287 | -0.263 |
| ARIMA(0,1,0)x(0,0,1)$_3$ | 0.674 | 0.675 | -0.393 | -0.388 |
| ARIMA(0,1,0)x(0,0,2)$_3$ | 0.661 | 0.664 | -0.410 | -0.401 |
| ARIMA(0,1,1)x(0,0,1)$_3$ | 0.653 | 0.656 | -0.422 | -0.413 |
| ARIMA(0,1,2)x(0,0,1)$_3$ | 0.641 | 0.645 | -0.439 | -0.425 |
| ARIMA(1,1,0)x(0,0,1)$_3$ | 0.647 | 0.650 | -0.432 | -0.422 |
| ARIMA(2,1,0)x(0,0,1)$_3$ | 0.634 | 0.638 | -0.450 | -0.435 |
| ARIMA(1,1,1)x(0,0,1)$_3$ | 0.629 | 0.633 | -0.458 | -0.443 |

The Box-Pierce Q for lags 48, 100, and 250 measuring randomness are satisfied with 95% confidence for the selected ARIMA(1,1,1) × (0,0,1)$_3$ model.

Plotting positions for the computed residuals $\hat{w}_t$ reveal that they are not normally distributed. In other words, the Box-Pierce goodness-of-fit, which is based on normally distributed $w_t$, is a measure for the goodness-of-fit only in a relative sense. In this case, the fitted parameters $\hat{\phi}$, $\hat{\theta}$, $\hat{\Theta}$, and the variance of residuals $\hat{\sigma}_w^2$ are least-squares estimates as opposed to maximum likelihood estimates. Nevertheless, the ACF and PACF in Figure 9, the variance of residuals $\hat{\sigma}_w^2$, and comparison of FPE, AIC, and BIC criteria altogether point toward a suitable model fit. The implication of $w_t$ being not normal, however, is to render the *l-step forecast*, defined as the conditional expectation $w_{t+l}^t = \mathrm{E}[w_{t+l}|w_t, w_{t-1},\ldots]$, and the *l-step forecast variance* $P_{t+l}^t = \mathrm{E}[(w_{t+l} - w_{t+l}^t)^2|w_t, w_{t-1},\ldots]$, insufficient for constructing the (1-$\alpha$) confidence or probability interval, because the first two moments are not sufficient to infer the probability density function as long as the residuals are not normally distributed. In this case, a nonparametric method is followed to fit a nonparametric probability density function to $w_t$. The premise of using the stochastic model (4.3) is that the future is statistically similar

to the past by preserving and reproducing the statistical characteristics of observed model errors.

### 4.2.2 Nonparametric Probability Distribution

Nonparametric methods are applied when parametric probability distributions fail to describe the stochastic sequence under consideration. Lall (1995) reviewed applications of nonparametric function estimation in hydrology. A probability density function of arbitrary shape can be locally approximated by a nonparametric model. This is particularly important when commonly used probability distributions (e.g., normal, log-normal, exponential, etc.) poorly fit the frequency of the observed stochastic series. However, despite their successful applications to hydrology, nonparametric approaches have the limitation that they do not extrapolate beyond the range of the record, since the sequence of future $w_t$ is hypothesized to have a similar nonparametric functional form of the fitted probability density function (PDF).

In parametric methods, the density function is estimated by assuming that data are drawn from a known parametric family of distributions. The methods of moments, maximum likelihood estimation, or any other methods are commonly used to estimate the parameters of the chosen PDF. In nonparametric approaches, a kernel function is often used to generalize the density function estimation. Given a set of $n$ observations $w_1$, $w_2$,…, $w_n$, a mathematical expression of a univariate kernel probability density estimator is ((e.g., Kim and Valdés, 2005)

$$\hat{f}_X(x) = \frac{1}{n\,h}\sum_{k=1}^{n} K\left(\frac{x - w_k}{h}\right) \tag{4.4}$$

where x is a random variable which stands for $w$; $K$ is a kernel function; $n$ is number of observations; and $h$ is a bandwidth that controls the variance of the kernel function. Kim and Valdés (2005) provide a list of kernel functions typically used in hydrology, the most widely used one being the Gaussian:

$$K(x) = \frac{1}{\sqrt{2\pi}} e^{-\frac{x^2}{2}} \tag{4.5}$$

An optimal estimate for the bandwidth for a Gaussian kernel is provided by Kim and Valdés (2005) citing Silverman (1986),

$$\hat{h} = \left(\frac{4}{3n}\right)^{1/5} \sigma \tag{4.6}$$

Where $\sigma$ is the standard deviation of the observed record, which in this case is equal to the standard deviation of observed residuals, $\hat{\sigma}_w \approx 0.79$. $n$ = 1028 is approximately the number of streamflow measurements in the calibration and validation period (7/1/2002-4/30/2005).

Note that the residual term $w_t$ in the error stochastic model (4.3) is not directly observed in the data sample $\varepsilon_1, \varepsilon_2, \ldots, \varepsilon_n$. This value can be approximated by assuming that $w_2 = w_1 = w_0 = w_{-1} = 0$ and then computing from (4.3)

$$w_k = \theta w_{k-1} + \Theta w_{k-3} - \theta\Theta w_{k-4} - (1+\phi)\varepsilon_{k-1} + \phi\varepsilon_{k-2} \tag{4.7}$$

for $k = 3, 4, \ldots, n$. Recall that the sequence $\varepsilon_1, \varepsilon_2, \ldots, \varepsilon_n$, which is used to construct the time series model (4.3), is computed from Eq. (4.1) using SWAT model simulations and corresponding streamflow measurements during the calibration and validation period.

Although the residuals $w_t$ have zero-mean and are independent, they do not follow any of the known parametric distributions. Figure 10 shows a relatively poor fit to the frequency histogram by Gaussian PDF assuming $w_t \sim N(0, \hat{\sigma}_w^2)$. The nonparametric fit (4.4) provides a remarkably improved local fit to the observed histogram.

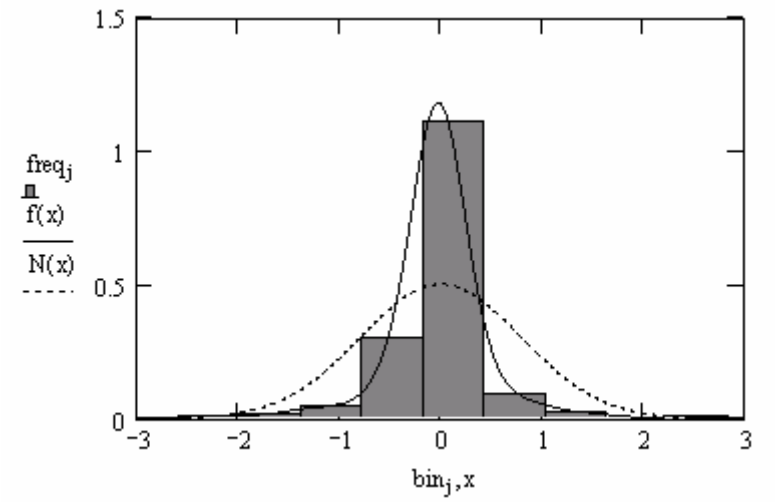


Figure 10. Frequency histogram, Gaussian PDF, and the nonparametric model fit to the computed series of residuals $w_k$. Both the histogram of residuals and normal distribution has zero mean and standard deviation $\hat{\sigma}_w$.

In the following section we now combine nonparametric random generation and Latin Hypercube Sampling (LHS) with the stochastic model (4.3) to synthesize the ensemble of model error time series $w_t$.

### 4.2.3 Nonparametric Random Generation

Random observations may be generated from probability distributions by making use of the fact that the cumulative probability function for any continuous variate is uniformly distributed over the interval [0, 1] (e.g., Haan, 2002). Thus, for any random variable $X$ with PDF $f_X(x)$, the variate $F_X(x)$

$$F_X(x) = \int_{-\infty}^{x} f_X(u)\,du \tag{4.8}$$

is uniformly distributed over [0, 1]. A procedure for generating a random value $x$ from $f_X(x)$ starts with generating a random number $R$ from the uniform distribution in the interval [0, 1], then setting $R = F_X(x)$, and finally solving for $x$ using the inverse relationship

$$x = F_X^{-1}(R) \tag{4.9}$$

Unfortunately, an explicit solution to (4.9) is not always possible because $F_X(x)$ may not be a simple function of $x$. The procedure for solving this equation is achieved in two steps. First, $F_X(x)$ is obtained by substituting the right-hand-side of (4.4) for $f_X(x)$ in (4.8) and commuting the order of summation with the integration operator. The term-wise integration can be carried either numerically or analytically in terms of resulting error functions. Secondly, for each randomly generated $R$, Eq. (4.9) is solved using any of the root searching techniques. The simple bisection method is used to obtain the root.

A large sequence of independent, identically distributed model residuals $w_t$ are randomly generated using the aforementioned procedure. Latin Hypercube Sampling (LHS) is employed as an efficient and effective alternative to conventional Monte Carlo sampling (MCS). The LHS (McKay et al. 1979) divides the CDF (i.e., the $F_X(x)$ function) into segments of equal width from each of which a random variate $R$ is generated. This way the whole CDF is covered, but with smaller number of replications than by MCS. LHS is more efficient than MCS at both ends of the CDF. The randomly generated sequence of $w_t$ is fed into Eq. (4.3) to synthesize ensemble time series of $\varepsilon_t$. As indicated at the outset, the computed $\varepsilon_t$ values, in fact, estimate the 3-day average as opposed to daily model prediction errors.

The generated ensemble of model errors together with the effect of precipitation uncertainty were used to construct an ensemble of flow duration curves based on a present land use map
(Figure 2a). However, before doing so, model forecast performance was first examined using the stochastic error model developed above and available streamflow data.

### 4.3 Model Forecast Evaluation

Figure 7 constitutes the first step in evaluating the model forecast performance during the post-validation period 5/1/2005-9/30/2005. The simulated streamflows and measured counterparts are daily and not 3-day averages. The relatively good fit indicated by extending the validation period further corroborates the calibrated model, and suggests that no further calibration is warranted. In general, the simulations somewhat overestimated measured streamflows during high flow periods and underestimated measured values during low flow periods.

To examine model forecast quality, the period from 7/1/2002 to 4/30/2005 (1035 days) is divided into two parts. The first 900 days (7/1/2002-12/16/2004) are used to construct the error model and the remaining 135 days from (12/16/2004-4/30/2005) are used for validation. The synthesized $\varepsilon_t$ values are subsequently added to SWAT model simulations conducted during the same time period to obtain an ensemble of model forecast (500 time series of streamflows),

$$\hat{o}_t = p_t + \hat{\varepsilon}_t \tag{4.10}$$

where the ^ symbol denotes an estimate. $\hat{o}_t$ is therefore considered as a surrogate to daily forecast of streamflows. Negative values of $\hat{o}_t$ computed from (4.10) are replaced with zero flow rates.

Thus, for each *t* (i.e., day), there are 500 values of computed streamflows, $\hat{o}_t$, available to construct uncertainty band (confidence interval). Figure 11 compares measured streamflow with $\hat{o}_t$. About 7% of observed values fall outside the 95% confidence band. Overall, the median of simulated 3-day average streamflows compared fairly well with the measured counterparts. The confidence band tends to be narrower for high flows and wider for low flows. This indicates that the forecast is more reliable during storm events and least reliable during smaller events and near base-flow conditions. To further examine model forecast during low flow conditions, the forecast evaluation period is extended to 9/30/2005. No significant storm events were recorded during the time period 5/1/2005-9/30/2005. While the simulated median daily flows generally compare well with measured counterparts, the 95% confidence band remains relatively wide (Figure 12). It is not clear if this is the result of inadequate error model fit or poor SWAT model performance during low flow periods. In general, watershed hydrologic models tend to perform poorer and have larger prediction uncertainty during low flow events (e.g., Hantush and Kalin, 2005). This phenomenon is largely attributed to the inadequacy of the models to capture the true intricate nature of runoff-subsurface flow interactions for small events. It will be shown later that simulated low flows generally have relatively high uncertainty.

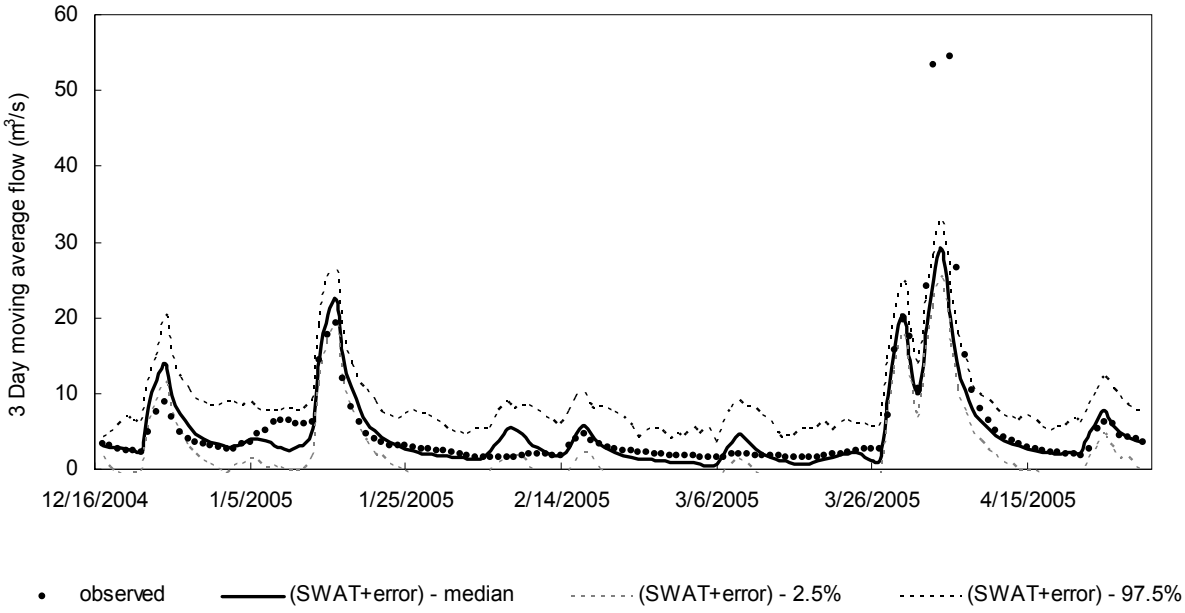


Figure 11. SWAT model ensemble forecast (median and 95% confidence band) and measured streamflows during the validation period (12/16/2004-4/30/2005). A total of 9 measurements lie outside the 95% confidence band (6.7 %). The simulated and measured values are 3-day averages.

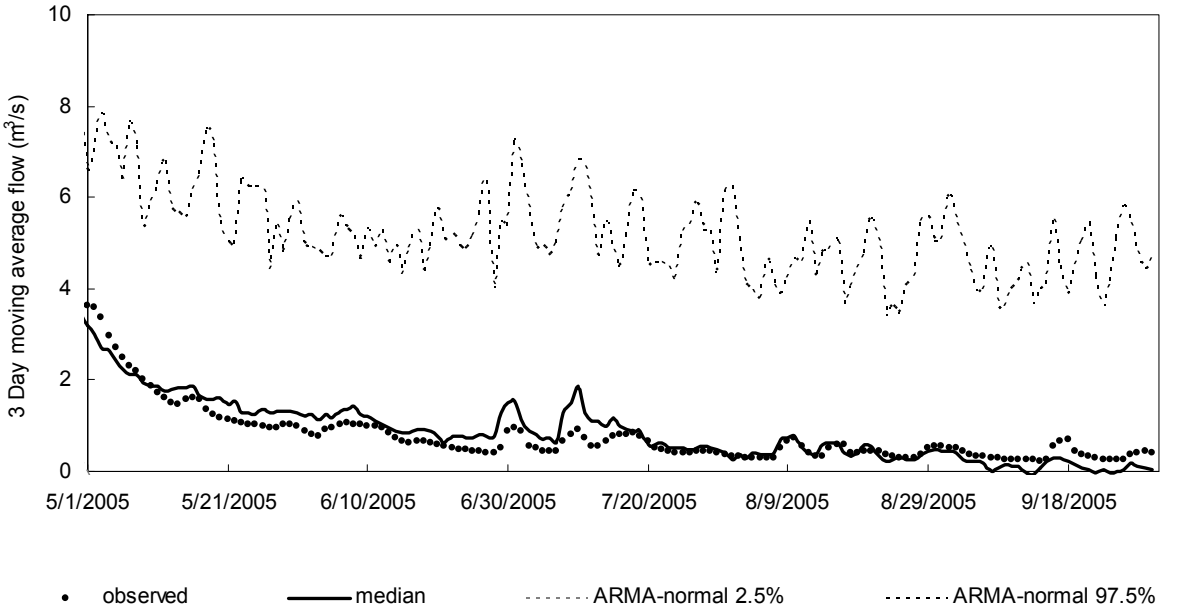


Figure 12. SWAT model forecast (median and 95% confidence band) and measured streamflows during the post-validation period (5/1/2005-9/30/2005). The simulated and measured values are 3-day averages.

Since a rationale was set to use the simulated 3-day average streamflows as surrogates to the daily flows, and for completeness, the ensemble forecast (median and 95% confidence

band) and measured daily flows are plotted in Figure 13. The median of 3-day average of the simulated streamflows appear to have grossly underestimated some of the measured peak flows. On the other hand, low flows were simulated fairly well.

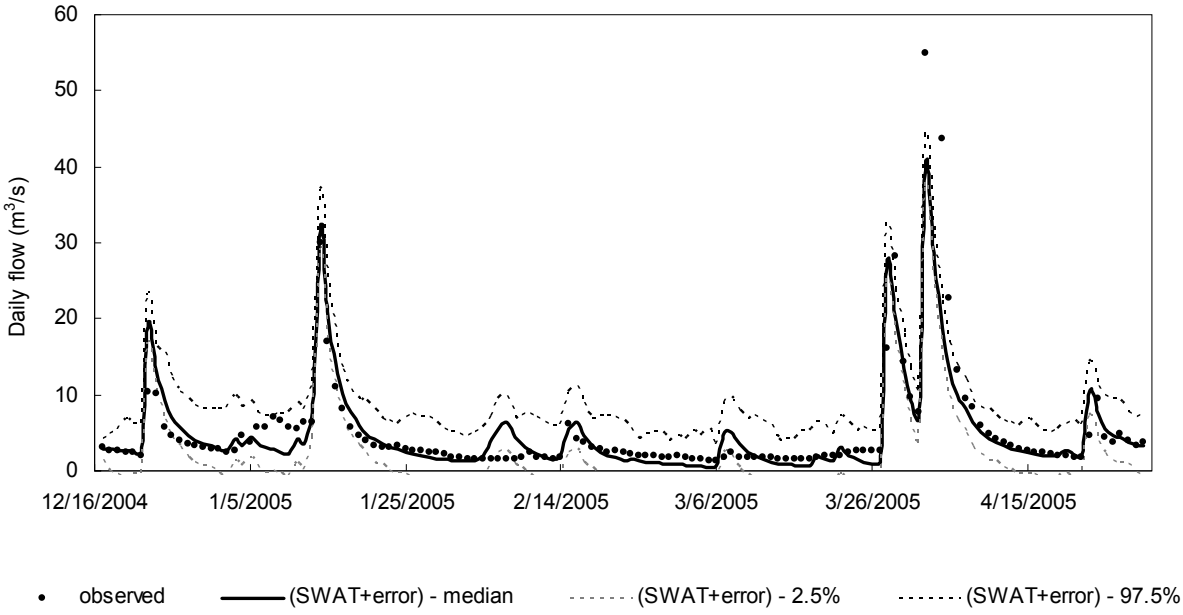


Figure 13. SWAT model 3-day average ensemble forecast (median and 95% confidence band) and measured daily streamflows during the validation period (12/16/2004-4/30/2005). A total of 15 measurements fall outside the 95% confidence band (11 %).

In the following subsection we present a methodology for computing SWAT model response to uncertainty associated with precipitation.

### 4.4 Uncertainty Due to Precipitation Variability

Precipitation is the central driver of most hydrological processes. Model results are highly sensitive to precipitation, and uncertainty in precipitation input may affect model output variability. Other sources of uncertainties, such as the combined effect of parametric uncertainty, model structural errors and measurement errors, are accounted for by the stochastic model (4.3). Precipitation temporal variability is addressed here.

For a rational analysis of the potential future impacts of the projected land use alterations on the hydrologic cycle of the Pocono Creek Watershed, it is essential to generate meteorological data for future conditions mimicking past conditions. Generated data such as precipitation, minimum and maximum air temperature, relative humidity, solar radiation and wind speed need to preserve statistics of past observations. Admittedly, the supposition of preserving the statistics of the past meteorological data ignores any global or local climate change effects. Thus, in this analysis, it is assumed that the anticipated changes in the

hydrologic regime are solely as a result of the projected modifications in the land use and land cover. SWAT has a built-in weather generator WXGEN (Sharpley and Williams, 1990) for atmospheric data generation. WXGEN relies on a first-order Markov-chain model to define wet and dry periods. For detailed information on weather data generation methodology, interested readers may refer to Kalin and Hantush (2006b). At the onset of this study, Mount Pocono station had daily atmospheric data from 10/1/1999 to 6/30/2005, which means that only 5 to 6 years of data was available to compute monthly statistics. At first glance, this duration may sound inappropriate for computing climate data statistics as the SWAT manual recommends the use of 20 years or longer data. Kalin and Hantush (2006b) investigated the adequacy of relying on a shorter duration data by comparison with rain data statistics pertinent to the Stroudsburg station, and showed that there are no significant differences in the statistics of the Stroudsburg station whether the past 5 years or 20 years of data is used. Therefore, for this specific application, it may be concluded that 5 years precipitation data reasonably reflects the statistics of a 20 years record for Pocono Creek.

## 4.5 Monte Carlo Simulations

To take into account the precipitation uncertainty, WXGEN is used to generate 500 sets of 20-year long records of daily precipitation assumed to represent precipitation from 1/1/2005 to 12/31/2024 based on averaged historical rainfall statistics at the Mount Pocono and Stroudsburg stations. A warm-up period from 1/1/1975 to 12/31/2004 of 30 years is used to eliminate the effect of uncertain initial conditions. Each of the synthesized time series of daily precipitation is fed into SWAT with the current land use map (Figure 2(a)) to obtain a 20-year long time series of daily streamflows. For each MC simulation, 3-day moving average is computed from the simulated daily streamflows. The MC simulation is repeated for a total number of 500, 20-year long time series of daily streamflows, from which the ensemble of 3-day averaged flows are computed.

Assuming that future simulations errors preserve the statistical characteristics of the historical record and follow the same stochastic model obtained in Eq. (4.3), an ensemble forecast of streamflows (median and 95% confidence band) for the period 1/1/2005 to 12/31/2024 is constructed by generating an ensemble of 20-year long sequences of $\varepsilon_t$ which then are added to the ensemble of MC simulations. In this manner, all sources of errors are accounted for in the forecast. The sequence of independent, identically distributed $w_t$ are randomly generated according to the procedure outlined in section 4.2.3, then used in conjunction with Eq. (4.7) to synthesize an ensemble of 500 20-year long sequences of daily (actually 3-day average) $\varepsilon_t$ values. The MC ensemble of 20-year long sequences of daily streamflows generated above are then corrupted by the randomly generated errors ($\varepsilon_t$) to obtain the ensemble forecast of streamflows at the USGS gauge station according to Eq. (4.10). It is worthwhile to note that the streamflows computed according to (4.10) constitute what is expected to be observed or measured rather than actual flow rates.

Summary statistics of some of the model outcomes for the current land use scenario are presented in Table 5. Mean, standard deviation (std), coefficient of variation (CV), median, and $2.5^{th}$ and $97.5^{th}$ percentiles (95% confidence interval) of the 500 realizations for each

flow statistics are given in the table to explicate uncertainty involved in the model outcomes due to precipitation as well as structural, parametric, and observation errors.

Table 5. Summary statistics of ensemble streamflow forecast based on most recent land use (Figure 2a). Values in the table are obtained from 500 time series of synthesized daily streamflows.

| | Average Daily Flow ($m^3/s$) (1) | Average Monthly Median Daily Flow ($m^3/s$) (2) | Average Monthly Maximum Daily Flow ($m^3/s$) (3) | Average Annual Maximum Daily Flow ($m^3/s$) (4) |
|---|---|---|---|---|
| mean | 2.42 | 2.10 | 7.12 | 17.39 |
| std | 0.203 | 0.182 | 0.411 | 1.93 |
| CV | 0.084 | 0.087 | 0.058 | 0.111 |
| median | 2.42 | 2.10 | 7.13 | 17.43 |
| 95% C.I | [2.02,2.80] | [1.75,2.45] | [6.35,7.91] | [13.91,21.82] |

NOTE: Daily flow here refers to 3 day moving average flow.

In the table, summary statistics related to high flow conditions as well as long term averages are given. The term “Average” in each column title denotes arithmetic average over the 20-year simulation period. For example, for each realization (i.e., time series) out of 500, daily flows are averaged over the 20-year simulation record to yield “average daily flow”. Thus, there are 500 such “average daily flow” values from which the mean, median, CV, and 95% confidence limits are computed. Average monthly-median of simulated daily streamflow in column (2) represents the arithmetic average over the simulation period of the median daily stream flows for each month and as indicated above is a required input to the PIFM wild brown trout habitat model. In column (3) the monthly maximum daily streamflows averaged over the simulation period are given. Column (4) shows the annual maximum daily streamflows averaged over the simulation period. Note that the summary statistics in Table 5 assume that the watershed remains undisturbed in the next 20 years, which obviously is contrary to what is anticipated. As such, they are hypothetical and are intended solely to provide insights into the effect of uncertainties on the interpretation of model predictions. Nevertheless, assuming that the land use/landscape in the watershed did not undergo significant changes in the past twenty years, the tabulated results may provide insights into the current flow conditions in Pocono Creek Watershed. The following remarks can be made from Table 5:

i. The average daily flow, average monthly median of daily flows, and average monthly maximum daily flow have small CV values and relatively narrower 95% confidence bands. Given all sources of uncertainty, these flow measures show small variability and appear to be reliable measures of flow characteristics.

ii. The average annual maximum daily flow shows a relatively greater uncertainty, as the larger CV and wider 95% confidence band indicate. The performance of flood control measures designed based on annual maximum daily flows should factor in the computed uncertainty.

iii. The low uncertainty associated with median monthly daily flow is rather encouraging given that it is an important parameter for the wild brown trout habitat (PIFM) model.

The ensemble characteristics of the simulated flow duration curves are depicted in Figure 14. The figure plots the median of the flow duration curves and the lower ($2.5^{th}$ percentile) and upper ($97.5^{th}$ percentile) limits of the 95% confidence interval. Each of the 500 synthesized $\hat{o}_t$ time series yielded one duration curve. A flow duration curve is a plot of the flow rate (say, $x$) versus probability of exceedance, P($X \geq x$). The return period, $T$, defined as the average recurrence interval between events equaling or exceeding a specified flow magnitude, $x$, is the reciprocal of P($X \geq x$): $T = 1/\ \text{P}(X \geq x)$. High flows are associated with small probability of exceedance, whereas low flows are associated with large probability of exceedance. The ensemble of flow duration curves in Figure 14 can be interpreted as follows. From the figure it can bee seen that for P($X \geq x$) = 0.002, daily streamflow at the gauge station is between 16 and 25 $m^3/s$ with 95% confidence. Since the corresponding return period is $T = 1/0.002 = 500$ days, this means that 500 day return period flow is between 16 and 25 $m^3/s$ with 95% confidence.

One may be lured into believing that uncertainty increases with increasing daily streamflow as the 95% confidence band gets wider with decreasing probability of exceedance, however, careful inspection of Figure 15 reveals that low flows have greater CV values and, thus, show much higher uncertainty than medium range and high flows. It is interesting to note that predicted streamflow rates ranging from about 2 to 11 ($m^3/s$) daily flow rates, corresponding to return periods of 2.5 and 50 days, respectively, have the smallest CV values and, therefore, lowest uncertainty. Higher flows with a recurrence period longer than 50 days have relatively higher uncertainty but much smaller than that associated with low flows, with return periods smaller than 2 days. Of course, these results are specific to Pocono Creek watershed.

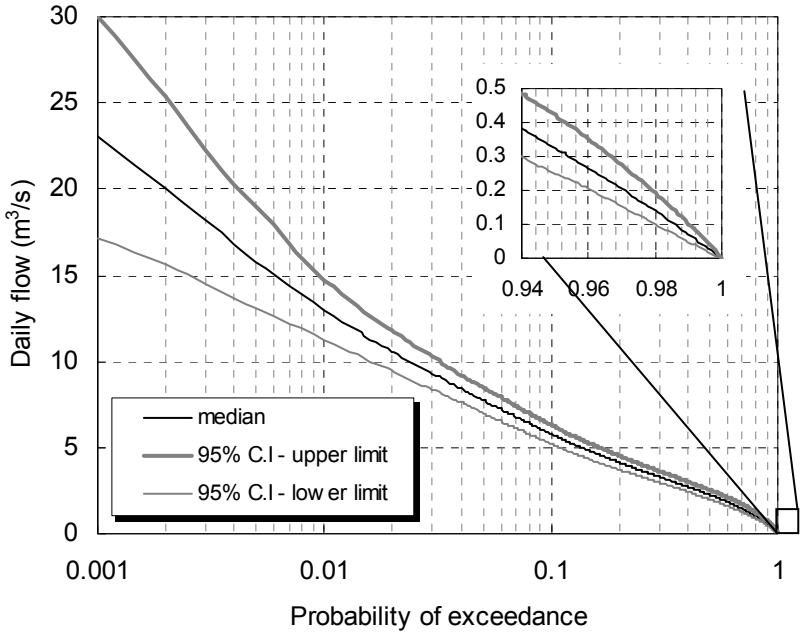


Figure 14. Median and 95% confidence band for the MC simulated duration curve. The flow duration curves are generated from 500 replicas of 20 years daily streamflows, $\hat{o}_t$.

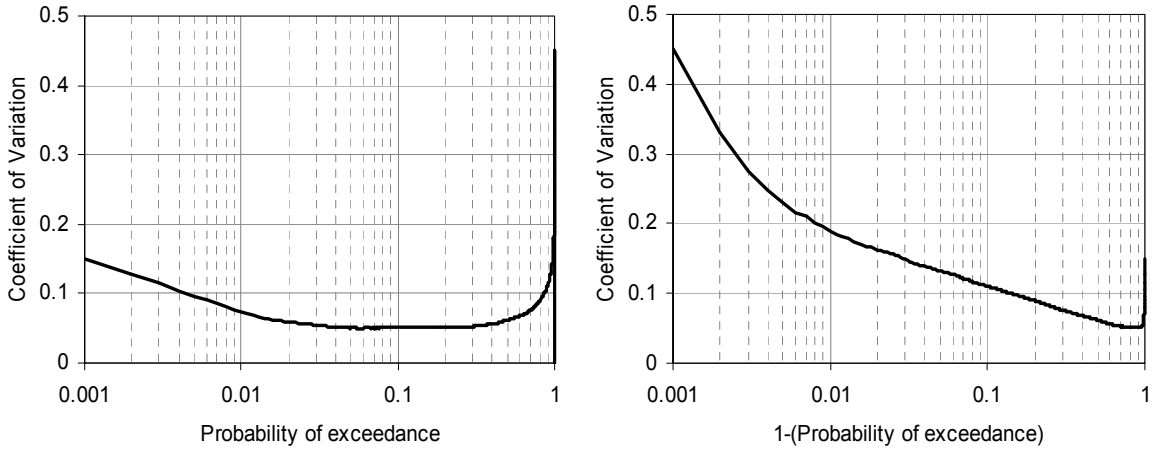


Figure 15. Coefficient of variation computed from ensemble of flow duration curves versus probability of exceedance in the left panel P($X \geq x$), and cumulative probability P($X \leq x$) in the right panel.

## 4.6 Conclusions

In this section model prediction capability was investigated using time series analysis and Monte Carlo-type Latin Hypercube simulations. Structural errors, parametric uncertainty, measurement errors, and rainfall variability together contribute to the SWAT model

predictive uncertainty. To minimize the effect of systematic SWAT prediction errors during significant events, 3-day averaged streamflows were considered as surrogates to daily flows. A stochastic model, which lumps the first three sources of errors, was developed by fitting ARIMA $(1,1,1) \times (0,0,1)_3$ time series model to 3-day averaged observed daily model errors during the calibration and verification period. A split-sample approach was implemented to construct and validate the error model. The stochastic error model allowed for constructing a forecast band (the median and 95% confidence band) for the SWAT model simulations. It was shown that most of the observed streamflows during the validation period (12/16/2004-4/30/2005) were within the 95% confidence band. The constructed model forecast was further evaluated using an additional set of measured streamflows during the period 5/1/2005-9/30/2005. Although the results showed consistency, the 95% confidence band was relatively wide due to the relatively low-flow period.

The effect of temporal precipitation variability was also accounted for using historical precipitation data recorded at the Mount Pocono and Stroudsburg stations. Synthesized precipitation rates by the SWAT built-in weather generator WXGEN along with MC simulation of the SWAT model and generated model errors all together were used to construct an ensemble forecast of daily streamflows for the next twenty years. It was shown that given all sources of model uncertainty, the average daily flow, average monthly median of daily flows, and average monthly maximum daily flow could be reliably predicted. The relatively low uncertainty associated with monthly median of daily flows indicate that this flow measure may be used reliably as an input to the brown trout habitat model (PIFM). Averaged over the simulated 20-years period, annual maximum daily flow showed relatively greater variability. The ensemble of daily flow duration curves was summarized by the median and 95% confidence band. The ensemble duration curve graph allows for the estimation of the daily flow range with 95% confidence for a specified design recurrence (return) period. SWAT simulated daily streamflow rates ranging from about 2 to 11 ($m^3/s$) showed least uncertainty. Computed daily streamflow rates below 2 $m^3/s$ had the greatest uncertainty, whereas for higher than 11 $m^3/s$, uncertainty was moderate. The higher uncertainty associated with low flows was not surprising as watershed models tend to perform relatively poorer during small events.

# 5 Impact of Land Use Changes

## 5.1 Introduction

Over the past 25 years, the population of the United States has grown over 30% (USDC Census Bureau, 2005). Naturally, such an ample growth in population leads to substantial increase in urbanized areas and results in a degradation and loss of forested and agricultural lands. Hydrologically, urbanization is accompanied by increased imperviousness in the landscape. Increase in impervious areas as well as reduction in soil permeability results in reduced infiltration rate, which means that more precipitation becomes surface runoff and less water is recharged to ground water. When increased surface runoff is combined with the effect of reduced surface roughness - a consequence of which is a shorter travel time - it is inevitable to observe more frequent and more intense local flood events. Such alterations in the flow regimes of streams and channels may lead to changes in channel morphology in the form of channel widening and deepening. On the other hand, groundwater recharge reduction results in the drop of groundwater levels and reduction of base flow to stream flow. Groundwater depletion can be further amplified due to an increase in groundwater withdrawal that accompanies population and economic growth. Consequently, stream flow is further depleted as groundwater levels are increasingly lowered by increased pumping. This could have undesirable ecological consequences not only due to limited available water, but also because of increase in pollutant concentrations and limited capabilities of the streams to dilute any toxic spills.

As indicated earlier, Monroe County, where the Pocono Creek is located, has the second fastest growing population in the state of Pennsylvania. By the year 2020, a 60% increase in Monroe County population is forecasted, and it is further projected that more than 70% of the Pocono Creek watershed will turn into commercial and residential areas, currently standing around 6% (Figure 16). The impact of population growth and urbanization on potential alterations in surface and groundwater regimes will be assessed through the modeling framework that has been developed.

## 5.2 Present Land Use Map and Future Build Out

A simulation period of 20 years, from 1/1/2005 to 12/31/2024, is employed to study the impact of changes in the land use on the hydrology of the watershed. Two land use scenarios are considered. First scenario (LU2000) assumes that land use pattern of the year 2000, as depicted in the top panel of Figure 16, is preserved during the simulation period. In the second scenario (LU2020) it is assumed that the build out would occur in 2020 or after (bottom panel in Figure 16). In both scenarios, land use pattern is assumed to remain the same throughout the 20 year simulation period. In other words, land use pattern is assumed time invariant during the course of the simulations. Ideally, it is desirable to let the land use pattern change gradually during the course of the simulations. However, this is not an easy task due to model limitations as this will require dynamic updating of land use related model parameters with time. Recall that the watershed model was calibrated and validated based on the land use pattern LU2000. The model setup for simulation of LU2000 is extended to

perform the model simulations of LU2020.

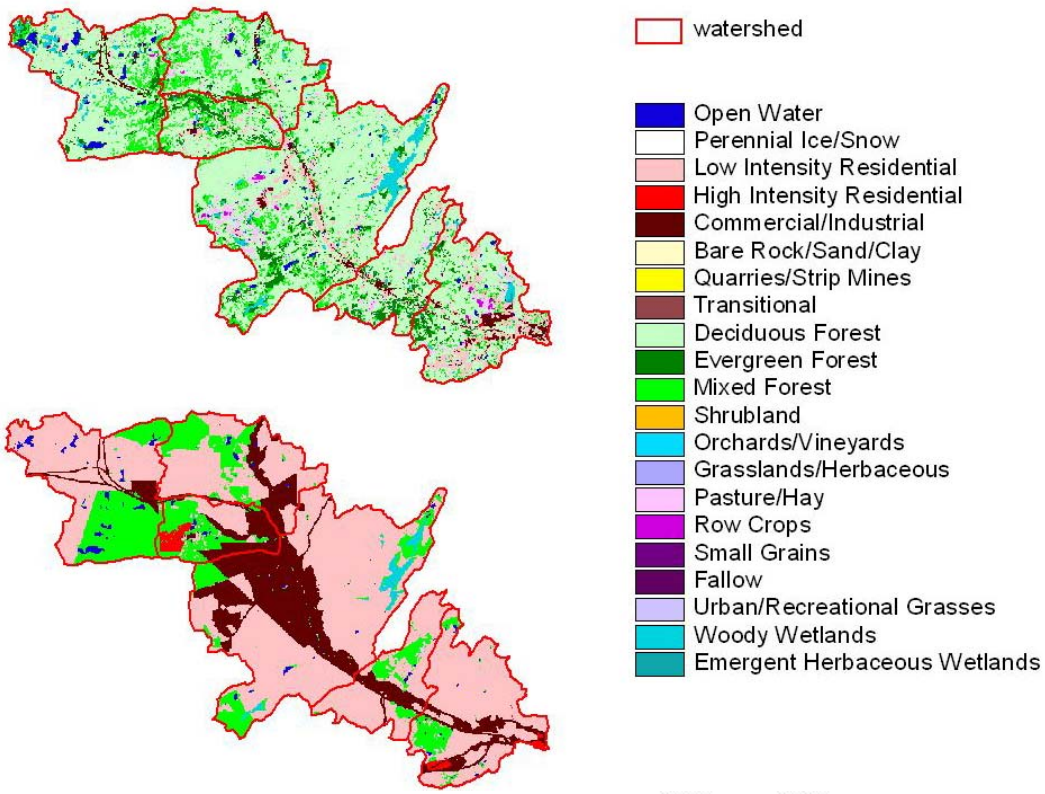


| LAND USE | 2000 (%) | 2020 (%) |
|---|---|---|
| Residential-High Density | 0.05 | 0.77 |
| Residential-Medium Density | - | 8.00 |
| Residential-Low Density | 3.53 | 44.19 |
| Commercial/Transportation | 2.25 | 22.84 |
| Pasture | 3.52 | 0.27 |
| Water | 1.43 | 1.43 |
| Wetlands | 3.80 | 3.80 |
| Forest | 85.23 | 18.70 |
| Agricultural Land-Row Crops | 0.19 | - |
| **TOTAL** | **100.00** | **100.00** |

Figure 16. Distribution of land use pattern in the Pocono Creek watershed in year 2000 (top) and the projected land use pattern for the year 2020 (bottom).

In simulating the effect of the two land use scenarios on streamflow characteristics all sources of model output error are neglected except rainfall variability; i.e., only SWAT model output $\hat{o}_t$ is considered, with the ensemble of rainfall rates generated for the period from 1/1/2005 to 12/31/2024. This is done primarily for two reasons. First, the error stochastic model (4.3) applies to LU2000, and it is therefore not conclusive if a similar error structure would apply to model simulations based on LU2020. Secondly, it is the relative

changes in the streamflow characteristics due to projected land use changes that are of concern rather than absolute predictions. Computed relative changes tend to have significantly lower uncertainty, consequently, they are much more reliable than absolute predictions of daily streamflows.

## 5.3 Monte Carlo Simulation

To take into account the precipitation uncertainty, we generated 50 sets of distinct daily precipitation records of 20 years length, each assumed to represent precipitation from 1/1/2005 to 12/31/2024. Measured precipitation data from 1/1/1975 to 12/31/2004 is inserted at the beginning of each record to obtain 50 precipitation input data files, each of which contain 50 years of daily precipitation. For each scenario, model simulations are performed for each of the 50 precipitation data files. A total of 2x50x50=5000 years of model simulations are performed at the daily time scale. Again, the first 30 years (1/1/1975 to 12/31/2004) of each realization is ignored for model warm-up purposes. Only the last 20 years of each realization are retained for further analysis. The reason for using the same measured precipitation data during the 30 year warm-up periods of all realizations is to minimize uncertainty relevant to initial conditions. Experimentation revealed that 50 realizations were adequate, and that more realizations had a negligible effect on the model outcome.

## 5.4 Predicted Changes in Streamflow

The MC simulations yielded 50 time series for each of the SWAT Model outputs that include, among others, stream flow, base flow, and groundwater recharge. Summary statistics of some of the model outcomes for the two scenarios, LU2000 and LU2020, are presented in Table 6 along with relative changes that might be expected when the land use pattern in the Pocono Creek Watershed changes from the one given in year 2000 to the one projected past year 2020. The statistics in the far left column and associated results in the table correspond to the variations of model output. Mean, standard deviation (std), coefficient of variation (CV), median, and $5^{th}$ and $95^{th}$ percentiles (90% confidence interval) for each design flow are computed from the resulting MC simulation and are given in the table to explicate uncertainty involved in the model outcomes due to precipitation. In the table summary statistics related to low and high flow conditions as well as long term averages are given. The first two columns given in the table are essentially base flow (BF) and stream flow (SF) averaged over the 20-year simulation period. The lowest computed flow occurring once every 10 years averaged over a 7-consecutive-day period (7Q10) listed in column (3) is widely used as a low-flow index in the United States (Smakhtin, 2001). This hydrologically-based design flow parameter is also used to protect against chronic effects by requiring that water quality criteria must be met at all times except during the 7Q10. Average monthly-median of simulated daily SF in column (4) represents the arithmetic average over the simulation period of the median daily stream flows for each month and as indicated above is a required input to the PIFM wild brown trout habitat model. In column (5) and (6) the monthly and annual maximum daily stream flows averaged over the simulation period are given, respectively.

Table 6. Summary statistics of computed streamflow characteristics at the USGS gauge station. The results are derived from 50 MC simulations each 20 years long.

| | | **Average BF ($m^3/s$)** (1) | **Average SF ($m^3/s$)** (2) | **7Q10 ($m^3/s$)** (3) | **Average Monthly Median Daily SF ($m^3/s$)** (4) | **Average Monthly Maximum Daily SF ($m^3/s$)** (5) | **Average Annual Maximum Daily Flow ($m^3/s$)** (6) |
|---|---|---|---|---|---|---|---|
| mean | LU2000 | 1.314 | 2.452 | 0.284 | 2.033 | 6.11 | 17.47 |
| | LU2020 | 0.911 | 2.426 | 0.252 | 1.829 | 7.40 | 20.86 |
| | % change | -30.6% | -1.1% | -11.1% | -10.1% | 21.1% | 19.4% |
| std | LU2000 | 0.071 | 0.137 | 0.054 | 0.108 | 0.450 | 2.28 |
| | LU2020 | 0.056 | 0.140 | 0.055 | 0.104 | 0.526 | 2.67 |
| CV | LU2000 | 0.054 | 0.056 | 0.191 | 0.053 | 0.074 | 0.131 |
| | LU2020 | 0.062 | 0.058 | 0.218 | 0.057 | 0.071 | 0.128 |
| median | LU2000 | 1.318 | 2.457 | 0.282 | 2.027 | 6.17 | 17.40 |
| | LU2020 | 0.909 | 2.431 | 0.242 | 1.826 | 7.47 | 20.81 |
| | % change | -31.0% | -1.1% | -14.4% | -9.9% | 21.0% | 19.6% |
| [5, 95]% | LU2000 | [1.205,1.421] | [2.232,2.682] | [0.197,0.364] | [1.852,2.207] | [5.35,6.71] | [13.59,22.31] |
| | LU2020 | [0.828,0.993] | [2.200,2.664] | [0.167,0.326] | [1.650,2.002] | [6.52,8.17] | [16.26,26.55] |
| | % change | [-31.3,-30.1]% | [-1.4,-0.7]% | [-15.2,-10.4]% | [-10.9,-9.3]% | [21.8,21.7]% | [19.6,19.0]% |

**mean**: Arithmetic average of 50 realizations

**std**: Standard deviation of 50 realizations

**CV**: Coefficient of variation (std/mean)

**median**: $50^{th}$ percentile of 50 realizations

**[5, 95]%**: $5^{th}$ and $95^{th}$ percentiles of the 50 realizations

**BF**: Base flow contribution to stream flow

**SF**: Stream flow

**7Q10**: Seven days average low flow with a 10 year return period.

**LU2000**: Simulations performed using land use coverage for year 2000

**LU2020**: Simulations performed using land use projections for 2020

**% change**: (LU2020-LU2000)/LU2000

Table 1 reveals the following observations and associated conclusions:

i. The mean value of 50 realizations for the average of simulated BF is expected to decline by 31%. This is simply due to reduced infiltration and consequently less recharge to the ground water. This reduction can be further aggravated if the effect of increased groundwater withdrawal due to higher water demand associated with population growth is imposed. To explore the effect of potential increase for groundwater demand, a more detailed groundwater flow model (MODFLOW) is being developed for the region by the USGS. In the simulations, groundwater pumpage is ignored. Precipitation uncertainty does not seem to impart much uncertainty on BF as CV is less than 0.1 for both

scenarios. The median, 5$^{th}$ and 95$^{th}$ percentiles are also expected to decline by the same rate as the mean.

ii. The average of simulated daily SF is relatively unaffected by urbanization. This can be explained on the basis that reduction in BF is offset by the increase in surface runoff. Yet, a negligible reduction (1.1%) in SF is observed. Mass balance of soil water dictates that average evapotranspiration (ET) is not impacted much by land use changes. Indeed, close examination of ET outputs from the model confirms this. Although forested areas have high transpiration (T), impervious surfaces have higher solar reflectivity, and thus higher evaporation (E). The reduction in (T) seems to be compensated by the increased (E). Similar to BF, uncertainty in precipitation has insignificant impact on SF. It should be noted that since the average of simulated daily SF is obtained by averaging simulated daily streamflows over the entire simulation record, it therefore does not represent actual daily flow conditions.

iii. On average, the computed 7Q10 is expected to decrease by almost 11%. This reduction can be attributed to the reduction in BF as low flows in perennial streams, such as Pocono Creek, are driven by BF which is predicted to decline by 31% on average over the study watershed. With 90% confidence, 7Q10 can be expected to be within the interval [0.197, 0.364] $m^3/s$ with the current land use conditions. With the projected land use conditions the 90% confidence interval for 7Q10 is [0.167, 0.326] $m^3/s$. The CV is estimated to increase by 14% due to changes in land use leading us to conclude that the combined effect of precipitation uncertainty and projected land use alterations are likely to cause higher uncertainty in 7Q10.

iv. Mean, median, 5$^{th}$ and 95$^{th}$ percentiles of average (i.e., averaged over the simulation period) monthly median of simulated daily SF as shown in column (4) are all reduced by about 10%. It is also clear from the table that the levels of uncertainties in both scenarios do not differ considerably, as they are only marginal. From a hydrologist's perspective, it is hard to reach a conclusion on how much risk this reduction poses to the brown trout population in Pocono Creek. Simulations based on the PIFM habitat model and the computed median flows will provide answers.

v. As expected, average monthly maximum of simulated daily SF increases as summarized in column (5). The expected increase is around 21% for mean, median, and 5$^{th}$ and 95$^{th}$ percentiles of the 50 realizations. Reasons for increase in peak flow magnitude as well as peak flow frequencies as a result of urbanization are well known: reduced infiltration rate and shorter travel times. The levels of uncertainties are about the same for both scenarios and can be deemed negligible with CV values of 0.07.

vi. Similarly, the increase in the average of annual maximum daily flow is anticipated with LU2020 projections. The mean and the median of average of annual maximum daily flow are predicted to increase by about 19%. The uncertainty associated with this design flow is the second highest after 7Q10, with a CV greater than 0.1. The 90% confidence band is estimated to increase from [13.59, 22.31] to [16.26, 26.55] in units of $m^3/s$.

In Figure 17, spatial distributions of the 20-year simulation average of annual groundwater recharge estimates [mm] at the subbasin scale are shown for the two scenarios. These are only model estimates, as real measurements of groundwater recharge are not

available. The figure delivers some important insights. There is a significant spatial variation of groundwater recharge in the watershed. Lower portions of the watershed (associated with lower elevations) have higher recharge rates than upper portions. When recharge estimates of the scenarios are compared, it is seen that with few exceptions almost all subwatersheds experience reduction of groundwater recharge. Another important observation is related to the extent of spatial variation of recharge in the two scenarios. In LU2000, the computed average recharge rates vary from 155 mm/year to 576 mm/year. In LU2020 the computed range of groundwater recharge is from 131 mm/year to 432 mm/year. This indicates that the projected land use change is expected to slightly reduce the spatial variation of groundwater recharge over the Pocono Creek watershed.

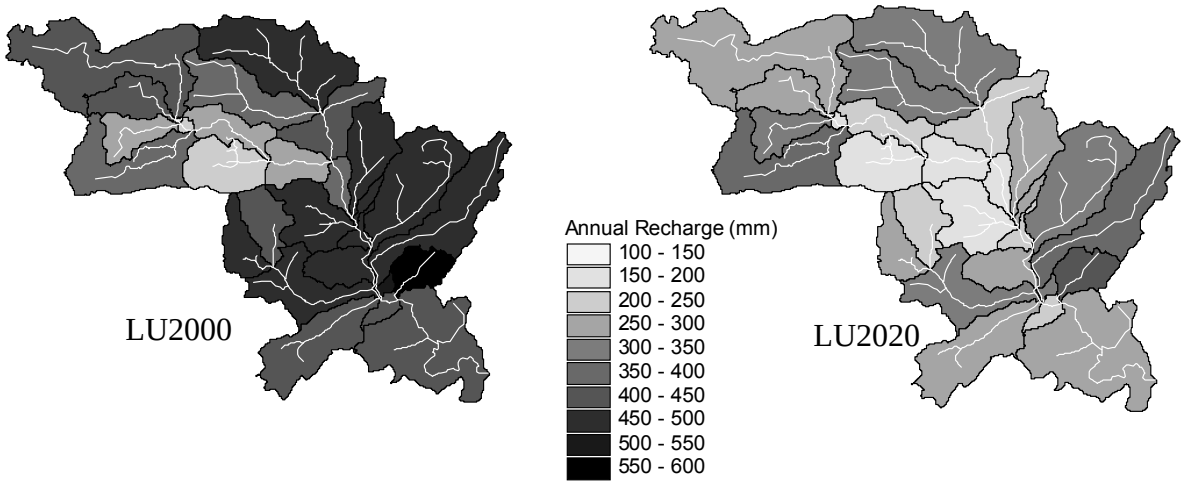


Figure 17. Annual groundwater recharge distributions in the Pocono Creek watershed for the two land use scenarios.

It should be noted that the results in Table 6 and Figure 17 assume that the build out in LU2020 occurs by 2020. The results would still characterize the watershed response even if the build out in LU2020 is presumed to occur after 2020. This may be true provided that pattern and variability of future precipitation remains unaltered.

The predicted annual groundwater recharge distributions depicted in Figure 17 were tabulated and passed on to USGS (Malvern, PA) to calibrate a quasi-three dimensional groundwater flow model (MODFLOW) for the watershed. The computed monthly median of daily flows were tabulated and passed on to the PA F&B Commission for use as input data to the brown trout habitat model (PIFM). Annual groundwater recharge averaged over the simulation record and spatially over the watershed was predicted to decline by 31%, from 424 to 292 mm/yr based on the LU2020 projections. The coefficient of variation (CV) of the computed annual groundwater recharge did not exceed 0.08, indicating fairly reliable model estimates thereof.

## 5.5 Predicted Changes to Flow Frequency and Duration

The medians of daily duration curves based on LU2000 and LU2020 are plotted in Figure 18. The probability of exceeding high flows and the risk for flood hazard are predicted to increase based on LU2020. On the other hand, flow exceeded at least 90% of the time (< 0.8 $m^3/s$) decreases in moving from LU2000 to LU2020, as depicted by the inner panel (Figure 18). Equivalently, this means that the chance for the flow to be less than or equal to a given low flow threshold increases. Therefore, base flows are likely to decrease with the projected land use changes. This is, of course, excluding the effect of the anticipated increase in groundwater withdrawals which will further decline base flows. Also note from Figure 18 that median flow due to LU2020 is slightly smaller than the one due to LU2000.

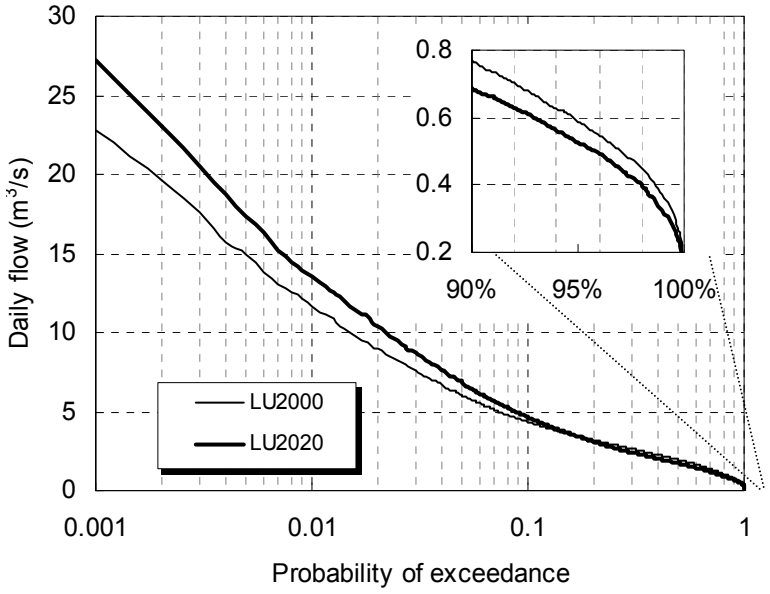


Figure 18. Median of the ensemble of the MC-simulated duration curves, bold thick line corresponds to simulations with LU2020, thin line corresponds to simulations with LU2000. The flow duration curves are generated from 50 replicas of 20 years of daily streamflows, $\hat{o}_t$.

## 5.6 Conclusions

The Pocono Creek watershed is threatened by high population growth anticipated over the next two to four decades. Potential effects of population growth and urbanization have heightened the need for implementing sustainable water resource management strategies in the watershed. In this section, potential hydrological changes in Pocono Creek due to anticipated build out in the watershed were investigated using the calibrated SWAT model and Monte Carlo simulations. Simulations accounted for anticipated rainfall variability over a 20 year period, with the current land use pattern and projected build out for the year past 2020, named LU2000 and LU2020, respectively. Simulation results revealed that on the average, daily base flow is expected to be reduced by 31%. The computed low-flow index, 7Q10, is expected to decline by 11% due to anticipated base-flow reduction. A metric for the

sustainability of fish habitat, the computed monthly median daily flow is expected to decline by 10% on the average. The monthly peak of simulated daily flows and annual maximum daily flow are expected to increase by 21% and 19%, respectively. The computed 7Q10 and average annual maximum daily flow showed relatively higher uncertainty than the other flow characteristics. Projected build out in the watershed is estimated to cause a significant decline in the annual groundwater recharge rates. The decline in the watershed-averaged annual groundwater recharge is predicted to be 31% based on LU2020 projections. The spatial variability of groundwater recharge appears to diminish with the projected urbanization in the watershed. In general, the likelihood that the watershed will experience high and low streamflows will increase with the projected urbanization, as indicated by the median of the MC simulated flow duration curves.

# 6 Critical Source Areas

## 6.1 Introduction

It is now evident from model predictions that the projected land use changes in the Pocono Creek watershed have the potential of increasing average annual maximum and average maximum monthly flows, and reducing 7Q10 and average median monthly daily flows at the watershed outlet. Informed management decisions may benefit from the identification of portions of the watershed that have the highest contribution to the reduction/increase in the quantity of interest. In a sense, preserving the land use of a particular area in the watershed can be considered as a best management practice (BMP). From this point of view, the problem can also be posed as identifying the locations of those BMPs that minimize the predicted changes. Of course, socioeconomic and policy matters may interfere with and preclude the implementation of a particular BMP, but knowing beforehand (i.e., before land development) critical areas in the watershed provides science-based guidance to the planning process.

There are limited applications in literature looking at the aspect of identifying or apportioning areas within a watershed based on their relative contributions to flow at the outlet. Saghafian and Khosroshahi (2005) address the same problem by focusing on flood source areas and they also emphasize lack of applications of this type. The approach adopted here, to be addressed shortly, has some similarities, however it differs from their work in two ways: i) in addition to high flows, the focus is extended to low and median flow characteristics (7Q10, monthly median daily flows), and ii) the focus here is not on individual event hydrographs, but rather on continuous flow time series.

## 6.2 Methodology

Let us assume that a given watershed is divided into *k* number of subareas, which will be referred as "elements" henceforth. There are two land use conditions, current (c) and future (f). The model run at the daily time scale with the future land use scenario for a given duration generates the flow time series $Q_t^f$ at the watershed outlet. Suppose that all the elements have the future land use/cover with the exception of element *j* retaining its present status. The generated flow time series at the outlet with this setup will be denoted as $Q_t^{f,j}$. For both flow time series, $Q_t^f$ and $Q_t^{f,j}$, the flow characteristics of interest, say F is computed and designated as $F^f$ and $F^{f,j}$ respectively. The following two indexes are defined to assess the relative impact of element *j* on the flow characteristic *F*:

$$\alpha_j = \frac{F^{f,j} - F^f}{F^f} \quad , \qquad \beta_j = \frac{\alpha_j}{A_j / A_w}$$

where $A_j$ and $A_w$ indicate areas of element *j* and the whole watershed, respectively. The first index, $\alpha_j$, signifies the absolute impact of element *j* on *F*. The second index, $\beta_j$, which is basically normalization of $\alpha_j$ with the percentage area of element *j*, measures the impact of land use changes in the element on *F* assuming these very changes occur over the entire watershed. In other words, $\beta$ is suitable for assessing the impact of land use changes per unit

area. By computing $\alpha_j$ and $\beta_j$ for $j$ = 1,..,$k$ one can rank the areas in the watershed from most critical to least. It is important to note that the order of ranking could be different not only depending on the index used but also depending on the flow characteristic of interest, $F$.

### 6.3 Results

As part of the modeling requirement, the Pocono Creek watershed was divided into 29 catchments, numbered from 1 to 29 with catchment 29 being the most downstream (Figure 19a). For management purposes this discretization might be too detailed. Hence, as an alternative we divided the watershed into 7 larger areas which are combinations of the 29 subbasins (Figure 19b). It should be noted that the larger areas correspond to the management areas in the pilot study (2001), with areas 4,5, and 6 in Figure 19(b) together falling within the management area 3 of the pilot study (Figure 20). Area 7 in Figure 19(b) overlaps with management areas 2 and 3 of the pilot study (Figure 20).

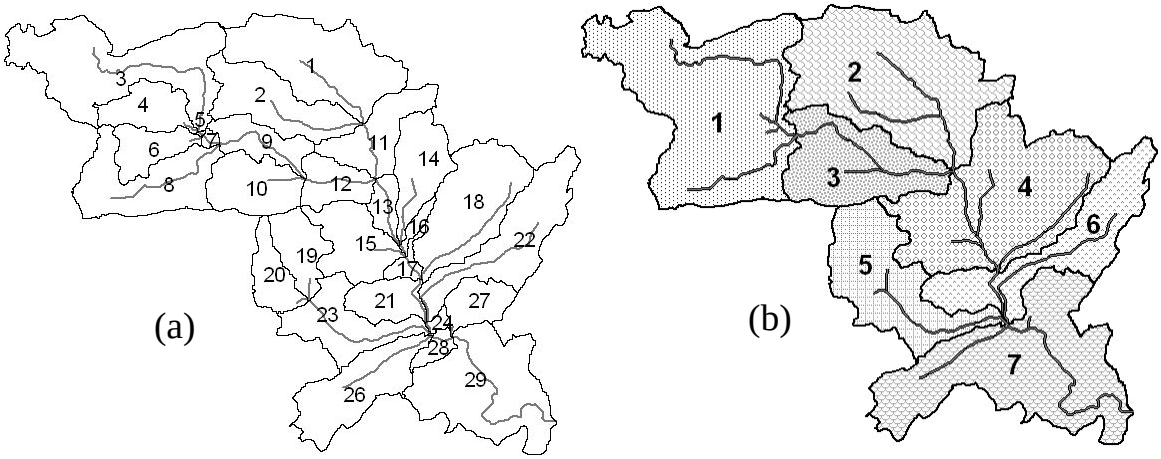


Figure 19. Watershed subdivisions used in determination of critical areas, (a) finer, (b) coarser.

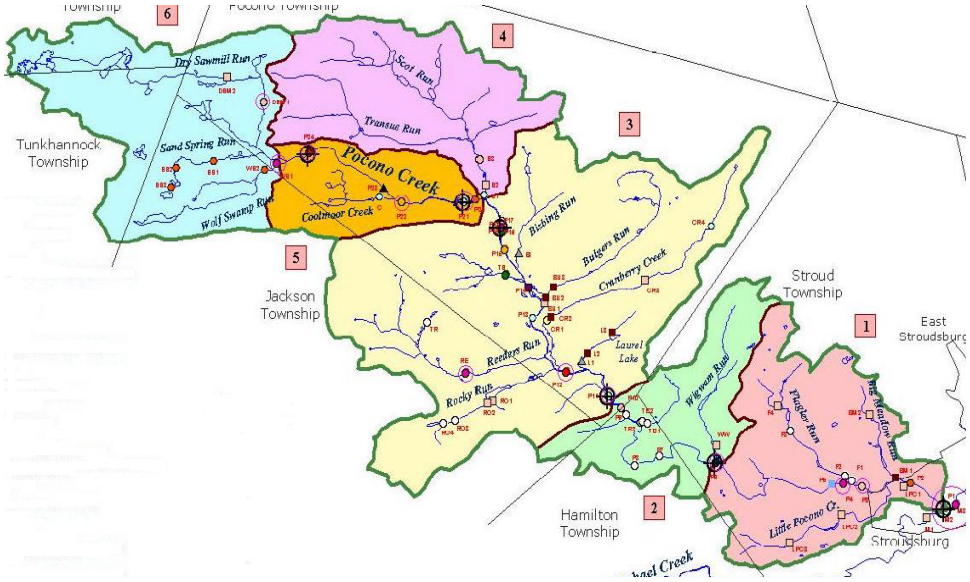


Figure 20. Management areas in Pocono Creek Watershed according to Pocono Pilot Study.

Table 7 summarizes the computed indices, $\alpha$ and $\beta$ with the coarser spatial scale for 7Q10, monthly median of daily flows and annual maximum daily flows, which divides the watershed into 7 drainage areas, $j$=1,..,7. Also given in the table are the rankings of each area for each index and flow characteristics. Figure 21 depicts these rankings on a gray scale spectrum for visual purposes. One immediate observation is that the rankings based on $\alpha$ and $\beta$ are quite consistent for monthly median of daily flows and annual maximum daily flow. Areas having the highest and lowest impact on these two flow characteristics do not change with the type of index. Management area 4 has the highest impact on the reduction of 7Q10 when $\alpha$ index is used, whereas management area 5 is the biggest contributor when $\beta$ index issued.

Table 7. Computed indices $\alpha$ and $\beta$ for the 7 management areas for 7Q10, monthly median of daily flows and annual maximum daily flows.

| | 7Q10 | | | | monthly median of daily flow | | | | annual maximum daily flow | | | |
|---|---|---|---|---|---|---|---|---|---|---|---|---|
| rank | $j$ | $\alpha_j$ | $j$ | $\beta_j$ | $j$ | $\alpha_j$ | $j$ | $\beta_j$ | $j$ | $\alpha_j$ | $j$ | $\beta_j$ |
| 1 | 4 | 8.58% | 5 | 0.54 | 4 | 2.55% | 4 | 0.15 | 7 | -5.48% | 7 | -0.32 |
| 2 | 7 | 7.15% | 4 | 0.51 | 7 | 2.51% | 7 | 0.14 | 4 | -3.88% | 4 | -0.23 |
| 3 | 2 | 6.18% | 7 | 0.41 | 2 | 2.03% | 2 | 0.12 | 1 | -2.47% | 6 | -0.22 |
| 4 | 5 | 4.95% | 2 | 0.35 | 1 | 1.97% | 5 | 0.09 | 6 | -1.96% | 1 | -0.11 |
| 5 | 1 | 3.60% | 6 | 0.22 | 5 | 0.85% | 1 | 0.09 | 2 | -1.69% | 2 | -0.10 |
| 6 | 6 | 1.95% | 3 | 0.17 | 6 | 0.73% | 6 | 0.08 | 3 | -0.56% | 3 | -0.07 |
| 7 | 3 | 1.47% | 1 | 0.17 | 3 | 0.59% | 3 | 0.07 | 5 | -0.50% | 5 | -0.05 |

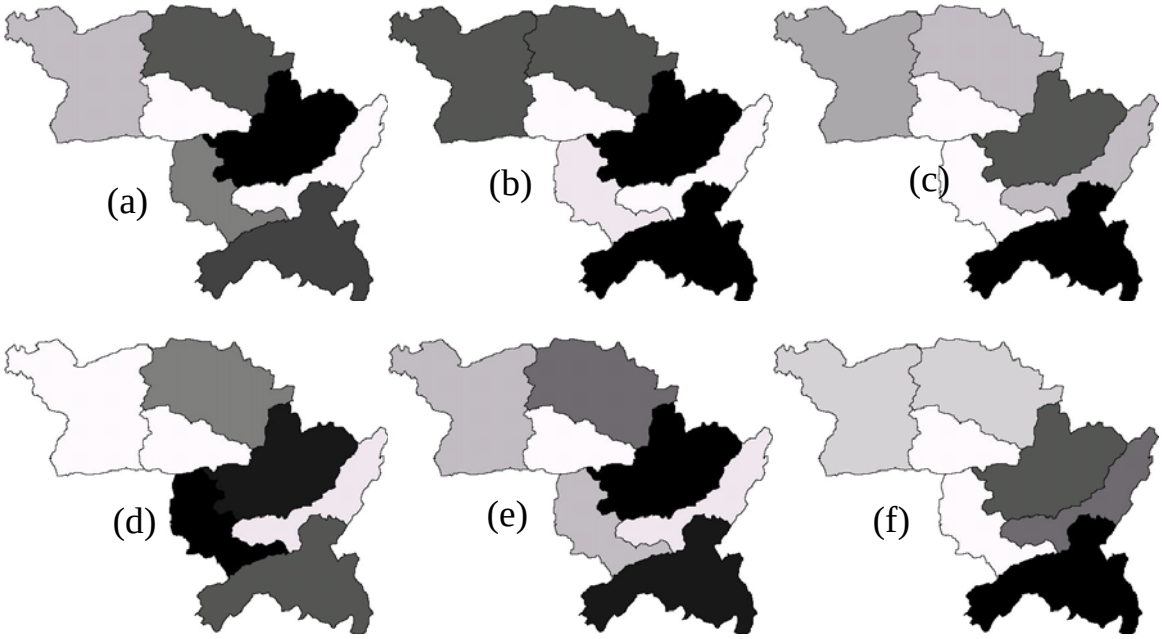


Figure 21. Ranking of the 7 management areas based on $\alpha$ (a, b, c) and $\beta$ (d, e, f) indices for 7Q10, monthly median of daily flows, and annual maximum daily flow, respectively.

Based on $\alpha$, area 4 (Figure 19(b)) is ranked first in terms of impact on 7Q10 and monthly median of daily flows, whereas areas 6 and 3 ranked the lowest, 6$^{th}$ and 7$^{th}$, respectively. Comparison of Figure 21 with Figure 17 reveals that area 4, through which Bisbing Run and Bulgers Run flow (Figure 20), contributes the highest annual groundwater recharge among the seven areas depicted in Figure 19(a). Since base flow is directly related to groundwater recharge, it is therefore expected that area 4 would have the highest impact on 7Q10. The predicted significant reduction in the annual groundwater recharge in area 4 due to projected land use changes (Figure 17) means a significantly greater fraction of precipitation would be available for runoff. This may explain area 4 being ranked first in terms of impact of land use changes on monthly median of daily flows, and ranked second for annual maximum daily flows.

Area 7 is ranked second based on $\alpha$ for its impact on 7Q10 and monthly median of daily flows, and first for annual maximum daily flows. Close proximity to the USGS streamflow gauge station (i.e., being downstream most), relatively high groundwater recharge rates, and the relatively larger area may be contributing to this ranking.

Significant portion of area 6 is occupied by wetlands (about 50%), which are maintained in both LU2000 and LU2020 as flow through features with zero infiltration. It is assumed that wetlands are preserved during land development. Therefore, groundwater recharge in area 6 is slightly reduced, thus, leading to least impact on 7Q10 and lowest ranking based on $\alpha$. Area 3, where the Camel Back Ski Area is located and Coolmoor Creek flows (Figure 20), is characterized by steep topography that is conducive to high runoff and low infiltration

regardless of the landscape features. This explains the lowest and second lowest ranking of area 3 with $\alpha$.

The ranking based on $\beta$ index is useful in assessing impacts when only portions of each of the 7 areas are planned to be developed. The most notable is area 5 which is ranked first for 7Q10 using $\beta$ index. With the exception of a small, steep northern portion, the area is topographically characterized by relatively low steepness and long slope length (Figure 1), and contributes significant groundwater recharge (Figure 17). Developments planned according to LU2020 may have the highest impact on 7Q10 if they occur within area 5.

## 6.4 Conclusions

The Pocono Creek watershed was divided into seven catchment areas and an index methodology was presented to rank the catchments' areas based on their impact on key streamflow characteristics due to anticipated land disturbances. The catchments' areas conformed to the six management areas in the pilot study (2001). Two indices were proposed. The first index, $\alpha$, signifies the absolute impact of a particular catchment area on the watershed response. The second index, $\beta$, is $\alpha$ normalized by the percentage area of the catchment, and therefore describes the impact of land use changes per unit area.

Using these indices, catchments' areas were ranked based on their potential to impact changes in the streamflow characteristics due to projected build out in the watershed. With a few exceptions, $\alpha$ and $\beta$ indices produced similar rankings among the 7 catchment areas for 7Q10, monthly median of daily flow, and annual maximum daily flow. Groundwater recharge, area, topographic features, and proximity to the streamflow gauge station may have contributed to the ranking results. The most downstream catchment, area 7, ranked first in terms of impact on annual maximum daily flows, and second in terms of impact on 7Q10 and monthly median daily flows. Catchment area 4, associated with the highest groundwater recharge, was ranked first and second based on $\alpha$ and $\beta$ indices, respectively, with regard to impact on 7Q10. In general, areas characterized by steep topography and significant wetlands ranked low, some times the lowest, with respect to impact on changes in the three design flows.

# 7 Summary and Conclusions

The Pocono Creek watershed, which is located in Monroe County, PA, is threatened by high population growth and urbanization. Of concern specifically is the potential impact of future developments in the watershed on the reduction of base flow and the consequent risk for degradation of wild brown trout habitats in Pocono Creek. Anticipated increase in imperviousness, on the other hand, is expected to elevate the risk for floods and the associated environmental damage. A watershed hydrologic modeling study was initiated by the U.S. EPA in collaboration with the U.S. Geological Survey and the Pennsylvania Fish and Boat Commission to assist Monroe County in planning for sustainable future developments in the Pocono Creek watershed.

Good application track-record of the SWAT model and its suitability to address watershed management problems led to the selection of the model to achieve the objective of quantifying the impact of anticipated land use changes on the hydrologic response of the Pocono Creek watershed. The model was successfully calibrated and validated for two sources of precipitation data, raingauge measured and radar estimated (NEXRAD). Two raingauge stations were available outside the watershed, but in close proximity to the perimeter. Simulated daily and monthly streamflows at the outlet compared fairly well to the observed values, for both sources of the rainfall data. The results reinforced the notion that NEXRAD is an effective source of spatio-temporal precipitation data and a viable alternative to the very costly installation, operation, and maintenance of a raingauge network. Future modeling studies in ungauged watersheds can be conducted with NEXRAD rainfall data.

Stochastic error propagation analysis was conducted using time series analysis and MC simulations to evaluate model predictive uncertainty. Model errors accounted for model structure uncertainty, parametric uncertainty, measurement errors, and rainfall variability. It was shown that the calibrated model was consistent in its forecast capability. MC simulations over a 20-year long period yielded an ensemble of rating curves of which the median and 95% confidence band of daily streamflows were plotted. These plots allow for the construction of the 95% confidence band for design flows corresponding to any given recurrence or return period. SWAT simulated daily streamflow rates in the range 2 to 11 ($m^3/s$) showed least uncertainty. Computed daily streamflow rates below 2 $m^3/s$ had the greatest uncertainty, whereas for higher than 11 $m^3/s$ uncertainty was moderate.

MC simulation over a 20-year period showed that the average daily base flow is expected to be reduced by 31% should the projected build out in the watershed occur. The computed low flow index, 7Q10 is expected to decline by 11%, and the monthly median daily flow is expected to be reduced by 10% on the average. Monthly peak of simulated daily flows and annual maximum daily flow were predicted to increase by 21% and 19% on the average, respectively. Groundwater recharge rate averaged over the watershed was predicted to decline by 31% due to the projected land use changes. The median of the MC simulated flow duration curves showed that, in general, the likelihood that the watershed will experience high and low streamflows will increase with the projected urbanization.

An index methodology was developed to rank seven subwatersheds - composing the modeled area of the Pocono Creek watershed - based on their relative impact on the watershed response to land developments. The first index, $\alpha$, signifies the absolute impact of a particular catchment area on the watershed response. The second index, $\beta$, is $\alpha$ normalized by the percentage area of the catchment, and therefore describes the impact of land use changes per unit area. With a few exceptions, $\alpha$ and $\beta$ indices produced similar rankings among the 7 catchment areas for 7Q10, monthly median of daily flow, and annual maximum daily flow. Groundwater recharge, area, topographic features, and proximity to the streamflow gauge station may have contributed to the ranking results. The most downstream catchment, area 7, ranked first in terms of impact on annual maximum daily flows, and second in terms of impact on 7Q10 and monthly median daily flows. Catchment area 4 associated with the highest groundwater recharge was ranked first and second for impact on 7Q10 based on $\alpha$ and $\beta$ indices, respectively. Areas characterized by steep topography (area 3) and significant wetlands (area 6) ranked low, some times the lowest, with respect to impact on the three design flows.

This model study predicted that low and high flows may, respectively, decrease and increase significantly as a result of urbanization. Land use changes in that part of the watershed where Bisbing Run and Bulgers Run flow through were predicted to have the highest impact on the reduction in low flows due to anticipated reduction in the groundwater recharge rates. The most downstream of the channel network, immediately upstream of the USGS gauge station, ranked first in terms of impact on monthly median of daily flow and maximum annual daily flow. Land disturbances in the topographically steep subwatershed, in which Coolmoor Creek flows, and the area that contains wetlands, through which Cranberry Creek flows, were predicted to generally have the least impact on the watershed response.

# 8 References


Arnold, J.G., and N. Fohrer. SWAT2000: current capabilities and research opportunities in applied watershed modeling. Hydrol. Process. 19: 563-572 (2005)

Arnold, J.G., Muttiah, R.S., Srinivasan, R., Allen, P.M. Regional estimation of base flow and groundwater recharge in the Upper Mississippi river basin. *J. Hydrol.* 227(1): 21-40 (2000).

Arnold, J.G., and P.M. Allen. Automated methods for estimating base flow and ground water recharge from streamflow records. *J. Am. Water. Resour. As.* 35(2): 411-424 (1999).

Arnold, J.G., Srinivasan, R., Muttiah, R.S., Williams, J.R. Large area hydrologic modeling and assessment part I: Model development. *Journal of the American Water Resources Association* 34(1): 73-89 (1998).

Arnold, J.G. and P.M. Allen. Estimating hydrologic budgets for three Illinois watersheds. *J. Hydrol.* 176(1): 57-77 (1996).

Arnold, J.G., Allen, P.M., Muttiah, R., and Bernhardt., G. Automated base flow separation and recession analysis techniques. *Ground Water* 33(6): 1010-1018 (1995).

Beven, K. and A. Binley. The future of distributed models: Model calibration and uncertainty prediction. *Hydrol. Process*. 6: 279-298 (1992).

Beven, K. and J. Freer. Equifinality, data assimilation, and uncertainty estimation in mechanistic modeling of complex environmental system using the GLUE methodology. *J. Hydrol*. 249: 11-29 (2001).

Binley A.M., K.J. Beven, A. Calver, and L.G. Watts. Changing Responses in Hydrology: Assessing the uncertainty in physically based model predictions. *Water Resour. Res*. 27(6): 1253-1261 (1991).

Borah, D.K. "Watershed scale non-point source pollution models: mathematical bases." In *Proceedings of the 2002 ASAE Annual International Meeting/CIGR World Congress*, Chicago, IL, 2002. Paper no. 022091.

Box, G.E.P., and G.M. Jenkins. "*Time Series Analysis, Forecasting, and Control*." San Francisco: Holden Day, 1970.

Carpenter, T.M. and K.P. Georgakakos. Impacts of parametric and radar rainfall uncertainty on the ensemble streamflow simulations of a distributed hydrologic model. *J. Hydrol*. 298: 202-221 (2004).

Di Luzio, M., Srinivasan, R., Arnold, J.G., and Neitsch, S.L. *ArcView interface for SWAT2000, User's Guide*, TWRI report TR-193. Texas Water Resources Institute, College Station, Texas, 2002.

Dilks, D.W., R.P. Canale, and P.G. Meier. Development of Bayesian Monte Carlo techniques for water quality model uncertainty. *Ecolog. Model*. 62: 149-162 (1992).

Eckhardt, K., and J.G. Arnold. Automated calibration of a distributed catchment model. *J. Hydrol.* 251:103-109 (2001).

Fohrer, N., Möller, D., and Steiner, N. An interdisciplinary modeling approach to evaluate the effects of land use change. *Phys. Chem. Earth* 27:655-662 (2002).

Freer J. and K. Beven. Bayesian estimation of uncertainty in runoff prediction and the value of data: An application of the GLUE approach. *Water Resour. Res*. 32(7): 2161-2173 (1996).

Green, W.H., and G.A. Ampt. Studies on soil physics, 1. The flow of air and water through soils. *J. Agr. Sci.* 4:11-24 (1911).

Haan, C.T. "*Statistical Methods in Hydrology*." Second Edition, Iowa State Press, A Blackwell Publishing Company. 496 pp. 2002.

Hantush**,** M.M., and L. Kalin. Uncertainty and sensitivity analysis of runoff and sediment yield in a small agricultural watershed with KINEROS2. *Hydrol. Sci. J* 50(6): 1151-1171 (2005)

Hossain, F., E.N. Anagnostou, T. Dinku, and M. Borga. Hydrological model sensitivity to parameter and radar rainfall estimation uncertainty. *Hydrol. Process*. 18: 3277-3291 (2004).

Hossain, F. and E. N. Anagnostou. Assessment of a probabilistic scheme for flood prediction. *J. Hydrolog. Engrng*. 10(2): 141-150 (2005)

Jha, M., Gassman, P.W., Secchi, S., Gu, R., Arnold, J.G., 2003. "Hydrologic simulation of the Maquoketa River watershed with SWAT." In *Proceedings of the AWRA 2003 Spring Specialty Conference*, Kansas City, MO, 2003.

Jayakrishnan, R., Srinivasan, R., Santhi, C., and Arnold, J.G. Advances in the application of the SWAT model for water resources management. *Hydrol. Process.* 19:749-762 (2005).

Kalin, L., and M.M. Hantush. Hydrologic Modeling of the Pocono Creek Watershed with NEXRAD and Rain Gauge Data. *J. Hydrolog. Engrng*. In press (2006a).

Kalin, L., M.M. Hantush. "Effect of Urbanization on Sustainability of Water Resources in the Pocono Creek Watershed." In *V.P. Singh and Y.J. Xu (ed.) Coastal Hydrology and Processes*, by American Institute of Hydrology, Water Resources Publications, 2006b, 59-70.

Kalin, L., M.M. Hantush. *Evaluation of sediment transport models and comparative application of two watershed models*, EPA/600/R-03/139. Cincinnati, OH: U.S. Environmental Protection Agency, 2003, http://www.epa.gov/ORD/NRMRL/Pubs/600r03139/600r03139.pdf.

Kim, T-W and J.B. Valdes. Synthetic generation of hydrologic time series based on nonparametric random generation. *J. Hydrol. Engrng*. 10(5): 395-404 (2005).

McKay, M.D., Beckman, R.J., and Conover, W. J. A Comparison of Three Methods for Selecting Values of Input Variables in the Analysis of Output from a Computer Code. *Technometrics* 21(2):239-245 (1979).

Lall, U. Recent advances in nonparametric function estimation: Hydrologic applications. *Rev. Geophys*. 33(S): 1093-1102 (1995).

Muleta, M.K., and J.W. Nicklow. Sensitivity and uncertainty analysis coupled with automatic calibration for a distributed watershed model. *J. Hydrol.* 306:127-145 (2005).

Nash, J.E., and Sutcliffe, J.V. River flow forecasting through conceptual models. Part 1: A discussion of principles. *J. Hydrol.* 10:282–290 (1970).

Neitsch, S.L., Arnold, J.G., Kiniry, J.R., Williams, J.R., and King, K.W. *Soil and Water assessment Tool Theoretical Documentation, version 2000*. TWRI report TR-191, Texas Water Resources Institute, College Station, Texas, 2002a.

Neitsch, S.L., Arnold, J.G., Kiniry, J.R., Williams, J.R., and King, K.W. *Soil and Water Assessment Tool User's Manual, version 2000*. TWRI report TR-192, Texas Water Resources Institute, College Station, Texas, 2002b.

NRC. "*Assessing the TMDL approach to water quality management*." Committee to Access the Scientific Basis of the Total Maximum Daily Load Approach to Water Pollution Reduction, Water Science and Technology Board, Division on Earth and Life Studies, National Research Council, Washington, D.C, 2001.

Pebesma, E.J., P. Switzer, and K. Loague. Error analysis for the evaluation of model performance: rainfall-runoff event time series data. *Hydrol. Process*. 19: 1529-1548 (2005).

Pocono Creek Pilot Study Draft Technical Report. *Geology, geomorphology, geohydrology, and surface water hydrology of the Pocono Creek Basin*, <http://www.state.nj.us/drbc/pocono_geology.PDF> (Jan. 30, 2006). Delaware River Basin Commission (DRBC), 2001.

Rallison, R.E., and Miller, N. "Past, present and future SCS runoff procedure." In *Rainfall runoff relationship*. *V.P. Singh, eds*., Water Resources Publication, Littleton, Colo., 1981, 353-364.

Saghafian, B. and Khosroshahi, M. Unit response approach for priority determination of flood source areas. *J. Hydro. Engrng.* 10(4): 270-277 (2005).

Saleh, A. and B. Du. "Application of SWAT and HSPF within BASINS program for the Upper North Bosque River watershed." In *Proceedings of the 2002 ASAE Annual International Meeting*, 2002.

Saltelli, A., K. Chan, and E.M. Scott. 2000. "*Sensitivity Analysis*." John Wiley & Sons, Ltd, 2000, 475 pp.

Santhi, C., Arnold, J.G, Williams, J.R., Dugas, W.A., Srinivasan, R., and Hauck, L.M. Validation of the SWAT model on a large river basin with point and nonpoint sources. *J. Am. Water. Resour. As.* 37(5):1169-1188 (2001).

Sharply, A.N., and J.R. Williams. Eds. *EPIC-Erosion Productivity Impact Calculator, 1. Model Documentation*, U.S. Department of Agriculture, Agricultural Research Service, Tech. Bull. 1768, 1990.

Shumway, R.H. "*Applied Statistical Time Series Analysis*." Prentice Hall, 1988, 379 pp.

Silverman, B.W. "*Density Estimation for Statistics and Data Analysis*." Chapman and Hall, New York, 1986.

Smakhtin, V.U. Low Flow Hydrology: A Review. *J. Hydrol*. 240:147-186 (2001).

Sophocleous, M., and S.M. Perkins. Methodology and application of combined watershed and ground-water models in Kansas. *J Hydrol.* 236:185-201 (2000).

Sorooshian, S. and J.A. Dracup. Stochastic parameter estimation procedures for hydrologic rainfall-runoff models: Correlated and Heteroscedastic error cases. *Water Resour. Res.* 16(2): 430-442 (1980).

Sorooshian, S., Gupta, V.K., and Fulton, J.L. Evaluation of maximum likelihood parameter estimation techniques for conceptual rainfall-runoff models: Influence of calibration data variability and length on model credibility. *Water Resour. Res.* 19(1):251-259 (1983).

Spear, R.C. and G.M. Hornberger. Eutrophication in peel inlet-II. Identification of critical uncertainties via generalized sensitivity analysis. *Water Res.* 14: 43-49 (1980).

Spear, R.C., T.M. Grieb, and N. Shang. Parameter uncertainty and interaction in complex environmental models. *Water Resour. Res*. 30(11): 3159-3169 (1994).

Srinivasan, R., Ramanarayanan, T.S., Arnold, J.G., Bednarz, S.T., Large area hydrologic modeling and assessment part II: model application. *Journal of the American Water Resources Association* 34(1): 91-101 (1998).

Tripathi, M.P., Panda, R.K., Raghuwanshi, N.S., and Singh, R. Hydrological modeling of a small watershed using generated rainfall in the soil and water assessment tool model. *Hydrol. Process.* 18:1811-1821 (2004).

US Department of Commerce, Census Bureau, Statistical Abstract of the United States, 2001. URL: http://www.census.gov/prod/2005pubs/06statab/pop.pdf, 2005.

USDA Soil Conservation Service. "National Engineering Handbook Section 4 Hydrology." Chapters 4-10, 1972.

Van der Perk, M. and M.F.P. Bierkens. The identifiability of parameters in a water quality model of the Biebrza, Poland. *J. Hydrol*. 200: 307-322 (1997).

Van Liew, M.W., Arnold, J.G., Gardbercht, J.D. Hydrologic simulation on agricultural watersheds: choosing between two models. *Trans. ASAE* 46(6): 1539-1551 (2003).

Williams, J.R. Flood routing with variable travel time or variable storage coefficients. *Trans. ASAE* 12(1):100-103 (1969).